lubricants

MDPI

Review

The Combined Use of Simulation and Friction and Wear Experiments in the Research of Green Lubricants

Xuan Yin [1,*], Dingyao Zhang [1], Haosheng Pang [2,3,*], Bing Zhang [1] and Dameng Liu [4]

[1] College of Mechanical and Electrical Engineering, Beijing University of Chemical Technology, Beijing 100029, China; zhangdingyao@buct.edu.cn (D.Z.); zhangbing@buct.edu.cn (B.Z.)
[2] Chinese Aeronautical Establishment, Beijing 100012, China
[3] National United Engineering Laboratory for Advanced Bearing Tribology, Henan University of Science and Technology, Luoyang 471000, China
[4] State Key Laboratory of Tribology in Advanced Equipment, Department of Mechanical Engineering, Tsinghua University, Beijing 100084, China; ldm@tsinghua.edu.cn
* Correspondence: yinxuan@buct.edu.cn (X.Y.); panghs.2020@tsinghua.org.cn (H.P.)

Abstract: During the operation of mechanical equipment, due to the intense friction among raw material or filler particles, there is conspicuous wear on the contact surfaces of components. Using green lubricants assumes a crucial role in mitigating the friction and wear, enhancing the equipment's service life and the production's reliability. This review centers on investigating the wear mechanism of green lubricants and undertakes a comprehensive summary and in-depth analysis of the research approach, integrating numerical simulation and friction and wear experiments. Moreover, the construction of the friction and wear testing machine and the intelligence of the testing system were probed, offering valuable design theories and research schemes for the development of effective anti-wear green lubricants.

Keywords: green lubricant; discrete element simulation; friction and wear experiment; wear

check for updates

Received: 12 May 2025
Revised: 8 June 2025
Accepted: 10 June 2025
Published: 11 June 2025

Citation: Yin, X.; Zhang, D.; Pang, H.; Zhang, B.; Liu, D. The Combined Use of Simulation and Friction and Wear Experiments in the Research of Green Lubricants. *Lubricants* **2025**, *13*, 259. https://doi.org/10.3390/lubricants13060259

Copyright: © 2025 by the authors. Licensee MDPI, Basel, Switzerland. This article is an open access article distributed under the terms and conditions of the Creative Commons Attribution (CC BY) license (https://creativecommons.org/licenses/by/4.0/).

1. Introduction

Green lubricants have the core characteristics of environmental friendliness, degradation, and high wear-resistance. There are various types of green lubricants: bio-based lubricants [1–3] (such as cellulose and vegetable oil), water-based lubricants [4,5] (such as ionic liquid and hydrogel), and nano-lubricants [6–8] (such as molybdenum disulfide (MoS_2), graphene, and silver). Cellulose, as a biopolymer material, possesses superior characteristics like biodegradability and environmental friendliness [9–11]. Various types of cellulose are prevalently utilized in the plastic processing and textile industry [12,13]. With the escalation of wear, the leakage during material advancement increases, reducing the output and causing cellulose materials to decompose. The polar ester groups of vegetable oils establish a dense boundary film through chemical adsorption, which significantly decreases the friction coefficient [14,15]. Their biodegradability and low ecological toxicity comply with environmental protection criteria and are especially suitable for sensitive working conditions. In addition, ionic liquid has two types: cationic (such as 1-alkyl-3-methylimidazolium salt) [16–18] and anionic (such as carboxylate salt [19,20] and phosphate ester salt [21,22]). In the boundary lubrication regime, polar ions establish a robust adsorption film on the surface of the metal substrate via Coulombic forces. Hydrogels can generate a fluid dynamic pressure effect reaching up to 1–3 GPa in the contact area [23,24]. Meanwhile, the interfacial water molecule layer exhibits an ultra-low shear strength and demonstrates excellent biocompatibility [25]. Nano-lubricants are

mainly composed of two-dimensional materials and nano-scale soft metals. MoS_2 [26–28] is particularly suitable for harsh environments such as a vacuum, high humidity, and high load (such as aerospace and vacuum machinery), making up for the shortcomings of traditional grease lubricants prone to volatilization or oxidation failure. Graphene is capable of attaining friction reduction and wear resistance via the interlayer sliding and vertical load-bearing within the two-dimensional layers [29–31]. This property can be further augmented through auxiliary functionalization modifications, such as nitrogen doping. Silver particles, with diameters ranging from 20 to 50 nm, can remarkably decrease the melting temperature via the size effect [32–34]. This allows for the repair of wear pits at relatively low temperatures.

In recent years, within the realm of research focused on enhancing the wear resistance characteristics of mechanical part surfaces using green lubricants, the simulation of mechanical equipment during operation and the tribological behavior of lubricants have emerged as two pivotal research areas. Regarding the simulation aspect, the discrete element simulation software, namely the event discrete element method (EDEM) [35–38], is currently considered a relatively advanced approach in solid mechanics simulation. This method enables the investigation of wear under diverse conditions, taking into account factors such as the configuration, speed, and material filling level. In the study of the tribological behavior of lubricants, the friction and wear testing machine serves as the primary testing apparatus. Aside from the commercially available friction and wear testing machines commonly employed by researchers, there are also custom-built friction and wear testing machines designed to meet the specific research requirements of various research groups. For self-made friction and wear testing machines, the design of the control systems is highly diverse. The upper and lower control systems cooperate through communication to collect data and control the execution components, thereby achieving precise control over experimental variables such as the load, speed, temperature, humidity, and other environmental factors. At present, a variety of control technologies have reached maturity, ensuring accurate regulation of experimental parameters.

Therefore, we undertake a comprehensive summary and in-depth analysis of the "integrated" design research approach that combines numerical simulation and friction and wear experiments, as shown in Figure 1. Firstly, it summarizes the research advancements regarding the lubrication properties and wear mechanism of green lubricants. Secondly, it focuses on the sliding process of green lubricants simulated using EDEM software (version 2022), investigating the wear distribution law on the contact surface based on the tribology outcomes. Finally, by summarizing the commercial friction and wear testing machines and self-built ones, the current development direction of intelligent friction and wear equipment based on the tribological research of green lubricants is proposed. With the assistance of the optimization of the measurement and control system of the friction and wear testing machine, it explores the wear condition of the micro-area. By studying the wear condition and wear distribution of green lubricants in the micro-area, this research aims to broaden the tribological research and development direction of green lubricants by promoting the research concept of integrating experiments and simulation. Meanwhile, it is expected to provide design concepts for enhancing the design methods of the lifespan of the equipment.

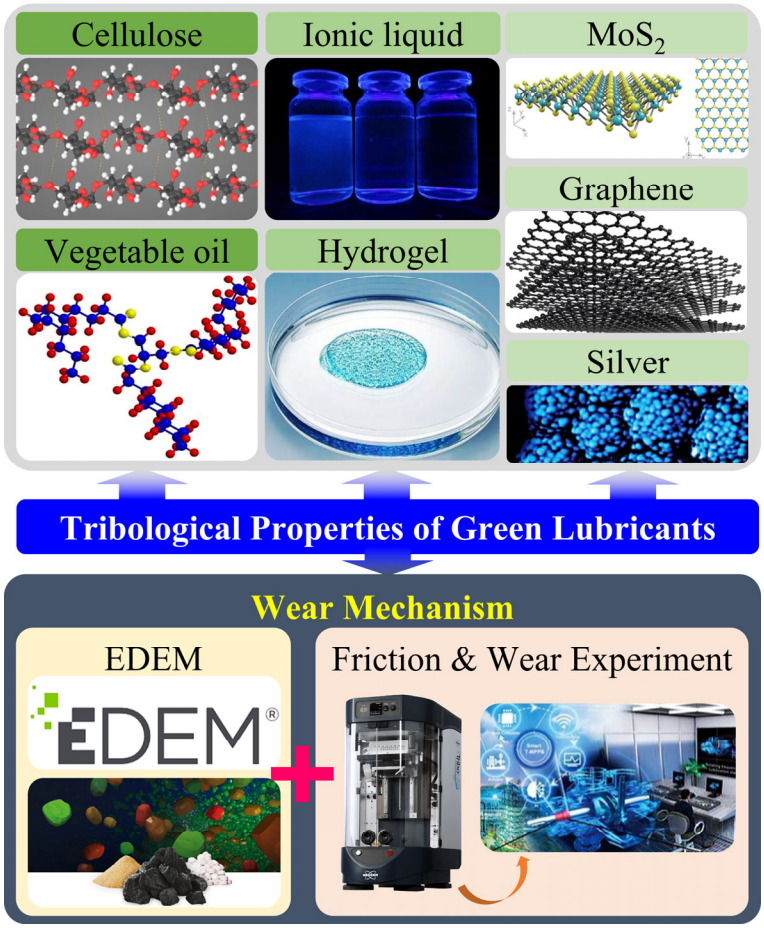


Figure 1. The combined system of simulation and friction-wear experiments for green lubricants.

2. Tribological Performances and Wear Mechanisms

2.1. Tribological Performances of Green Lubricants

2.1.1. Green Lubricants Based on Bio-Based Lubricants

- Cellulose

Cellulose fibers are natural organic base polymers that demonstrate good resilience after undergoing frictional forces when utilized as matrix materials [39], presenting high efficiency in reducing wear and stabilizing friction coefficients [40–42]. Cheng et al. [43] significantly enhanced the tensile strength and modulus of starch by employing cellulose nanocrystals, cellulose nanofibers, and micro-fibrillated cellulose, achieving a 242% increase in tensile strength and a 416% increase in modulus. Our research group also discovered a hybrid carbon nanosheet formed through orientation-driven hydroxypropyl methylcellulose (HPMC) decomposition [44,45], which created a mixed nanosheet transfer film containing organic chains on the sliding contact surface, attaining an interface state of ultra-low wear. Additionally, our research group investigated the influence of contact stress on the across-scale tribological properties of cellulose [46], revealing that the wear mechanisms of the low-speed group showed slight adhesive wear. Cellulose is frequently employed as a filler in the reinforcement modification of base materials to enhance the tribological properties. Wang et al. [42] fabricated ultra-high molecular weight polyethylene composite materials doped with nanocellulose through ball milling and hot pressing, with nanocellulose functioning as a lubricating phase to lower the friction coefficient of the matrix. Lin et al. [10] incorporated nanocellulose into a natural/isoprene mixed rubber matrix through mechanical blending, leading to a remarkable decrease in the friction coeffi-

cient and wear rate. Mohit et al. [47] extracted nanocellulose from sugarcane bagasse via mechanical means to reinforce epoxy resin, confirming that nanocellulose can effectively enhance the wear resistance of the resin matrix.

Research on cellulose as a green lubricant demonstrates significant potential within the realm of tribology. Nevertheless, its practical application still confronts several crucial limitations. Firstly, the rigid structure and weak interfacial adsorption of cellulose molecular chains impede the formation of a continuous and stable lubricating film on the surface of friction pairs. Notably, under boundary lubrication conditions, the cellulose film layer is highly susceptible to shear failure. Moreover, the ultimate load it can withstand is substantially lower than that of traditional mineral lubricants. Secondly, cellulose exhibits a relatively low glass transition temperature, and the temperature range for thermal degradation is narrow (approximately 200–300 °C). At elevated temperatures, molecular chain degradation or carbonization readily occurs. This leads to a sharp rise in the coefficient of friction and exacerbates abrasive wear, rendering it difficult to meet the thermal management requirements of high-speed and high energy-consuming systems. Finally, despite cellulose possessing excellent biodegradability, it is highly vulnerable to microbial degradation or hydrolysis in open systems. This ultimately results in a shortened lubrication lifespan.

- Vegetable oils

Vegetable oil, serving as the base oil for green lubricants, owes its core frictional advantage to the characteristics of its molecular structure, specifically long-chain fatty acid esters. Based on the fatty acid structure, vegetable oils can be categorized into the high oleic acid type (like sunflower seed oil), the polyunsaturated type (like soybean oil), and the functionally modified oils (those modified via epoxidation and thiolation). Stradolini et al. [48] carried out modifications on castor oil and epoxidized soybean oil via transesterification, transamidation, and epoxy ring-opening reactions. They discovered that the transamidated castor oil polyol exhibits a high viscosity index, excellent oxidation stability, and environmental friendliness, thus holding broad application prospects in the realm of bio-lubricants. Arumugam et al. [49] discovered that chemically modified rapeseed oil-based bio-lubricants exhibit excellent oxidation stability, enhanced low-temperature fluidity, and advantages regarding friction force and friction coefficient. Subsequently, Arumugam et al. [50] explored the feasibility of utilizing rapeseed oil-based bio-lubricants as substitutes for petroleum-based synthetic lubricants. Their findings indicated that bio-lubricants with the addition of nano-CuO can mitigate the wear of metal substrates. Yao et al. [51] reported that 2,3-Butanediol monooleate and 2,3-Butanediol dioleate possess a very high viscosity index and remarkable low-temperature resistance. These molecules have the potential to emerge as new ideal bio-lubricants, and their functional characteristics can be tailored through targeted structural synthesis. Matiliunaite et al. [52] found that saturated acids can enhance the oxidation stability and lubricity of bio-lubricants. Bhowmik et al. [53] enhanced the tribological properties of high oleic soybean oil (HOSO) by converting unsaturated fatty acids into saturated fatty acids through a novel chemical modification approach. This chemical modification process led to an approximate 10% increase in the wear resistance of HOSO at both room temperature and 100 °C. Sankaran et al. [54] conducted an experiment where they blended sesame oil with spherical TiO_2 and rod-shaped ZnO. Their findings indicated that the friction coefficient and wear scar diameter were decreased by 24.04% and 13.74%, respectively. Avilés et al. [55] modified peanut oil lubricant by incorporating the ionic liquid diethylmethylammonium methylsulfate. The results showed that the friction coefficient of the newly developed bio-lubricant was reduced to 0.080, and the wear rate was decreased by up to 96.3%. Nagendramma [56] synthesized pentaerythritol tetraoleate by using pentaerythritol and oleic acid as starting

materials and ion exchange resin Indion-130 as a catalyst. This product exhibits promising potential as a base oil for extreme pressure industrial gear oil VG-68.

Vegetable oil-based lubricants have found applications in the mechanical domain. For example, in Europe, rapeseed oil and sunflower seed oil are predominantly utilized in the development of hydraulic oil and gear oil. Correspondingly, the Danfoss Company in China has introduced castor oil-based bio-lubricant for commercial vehicles. Nevertheless, the application of vegetable oils remains primarily concentrated in medium and small load conditions (such as in agricultural machinery and food machinery), and several key issues exist: firstly, the residual C=C double bonds give rise to oxidation; secondly, the ester bonds are susceptible to hydrolysis, which accelerates corrosion; thirdly, traditional additives exhibit poor compatibility with vegetable oils and contravene environmental protection principles; fourthly, there is a dearth of frictional testing standards for vegetable oil lubricants in China. Notwithstanding these challenges, vegetable oils, as green lubricants, also present significant development opportunities. China's "carbon neutrality" objective and the European Union's "Green Deal" have spurred demand for environmentally friendly lubricants. The automotive industry is expediting the adoption of minimum quantity lubrication (MQL) technology, thereby creating high-end application scenarios for vegetable oils. Through novel molecular design and the development of intelligent additives, it is possible to strike a balance between low-temperature fluidity and high oxidation stability and to extend the service life of equipment.

2.1.2. Green Lubricants Based on Water-Based Lubricants

- Ionic liquid

Ionic liquids have emerged as a research focus in green lubricants owing to their molecular designability, low vapor pressure, and outstanding thermal stability. In recent years, tribological research has been concentrated on the following areas: enhancing lubrication performance, achieving synergistic effects, and adapting to extreme conditions. Li et al. [57] discovered that the lubricating performance of 1-ethyl-3-methylimidazolium tetrafluoroborate ionic liquid could be actively regulated by applying an electric current. Concurrently, the addition of Fe_3O_4 nanoparticles further enhanced the lubricating effect of the ionic liquid under high current intensity. Sadeghi et al. [58] examined the influence of 1-ethyl-3-methylimidazolium diethylphosphate ionic liquid on the tribological properties of diamond-like carbon films and found that a composite lubrication system of solid and liquid could generate beneficial synergistic effects. Han et al. [59] synthesized oxygen-containing ionic liquids with low chemical activity and excellent adsorption performance. The lubrication mechanism is the formation of an inorganic–organic double friction film composed of a metal oxide layer and an organic layer on the friction contact surface, which can be utilized to lubricate magnesium alloys. Wang et al. [60] integrated carbon dots and ionic liquids to acquire carbon dot-based ionic liquids (CDILs) and discovered that CDILs exhibited the optimal corrosion resistance and lubrication performance. The team further carried out ionic modification on the carbon dots via organic ammonium cations [61], augmenting their lubricating performance at both room temperature and high temperatures, providing significant protection to the steel surface. Zuo et al. [62] combined ionic liquid with MoS_2, reducing the friction coefficient to 0.024. Likewise, Li et al. [63] integrated ionic liquid with graphene oxide to form a more stable polar adsorption and tribochemical reaction film, reducing the coefficient of friction by 89.7%. These studies suggest that the morphological design is of vital significance for synergy. Additionally, simulation also assumes a crucial role in the investigation of the lubricating performance of ionic liquids, offering novel ideas for the molecular design of lubricants. Zhang et al. [64] revealed via molecular dynamics that during processing, the ionic liquid combines with

the surface texture. Compared to traditional lubricants, it can lower the cutting processing temperature and abrasive wear. Qu et al. [65] Investigated the lubrication performance of ionic liquids in vacuum and air environments by integrating in situ quadrupole mass spectrometry and molecular dynamics simulation. It was discovered that ionic liquids containing hydroxyl groups exhibit stable lubrication performance in both air and vacuum, fulfilling the requirement for high-end lubricants in extreme circumstances.

Ionic liquids exhibit unique lubricating properties; however, their applications in the friction field still face certain limitations. Firstly, the cations and anions of ionic liquids tend to undergo electrochemical reactions with metal surfaces, thereby causing corrosion of the metal surfaces. Additionally, some ionic liquids are liable to decompose under high-temperature or oxidation conditions, producing acidic byproducts that further exacerbate the corrosion issue. Secondly, ionic liquids display poor compatibility with poly-α-olefins and mineral oils. To enhance their oil solubility, it is often necessary to rely on designs featuring long alkyl chains or protonic structures. Thirdly, the thermal stability of ionic liquids is constrained by their chemical compositions. Moreover, the synthesis procedures of ionic liquids are intricate, and the raw materials are costly. Most significantly, their biodegradability and environmental safety have not been comprehensively determined. In the future, further in-depth exploration can be conducted on aspects such as the customization of molecular structures, the formulation of lubrication systems, and the greenification of synthesis processes. This will enable the achievement of technological breakthroughs and effectively meet the requirements of green industrial lubrication.

- Hydrogels

The core advantage of hydrogels serving as a green lubricant resides in their capacity to attain ultra-low friction (with a friction coefficient as low as 0.02) via the interfacial hydration layer and the biomimetic lubrication mechanism. Hydrogels are categorized into physically crosslinked (formed via hydrogen bonds or van der Waals forces) and chemically crosslinked types (formed through covalent bonds) [66–68]. The three-dimensional network structure of hydrogels imparts elastohydrodynamic lubrication properties to them. These features render hydrogels an ideal lubricating medium for artificial joints and other medical devices. Yan et al. [69] fabricated polyelectrolyte hydrogels capable of forming nanoscale lubricating layers via surface-induced self-assembly. Under a 2 N load, the friction coefficient could reach 0.02, and the lubrication performance could be sustained for 500 days. Hafezi et al. [70] explored injectable and thermosensitive agarose hydrogels as carriers for hyaluronic acid. By establishing a three-dimensional polymer network, the adjacent surfaces of the bearing were separated, leading to a reduction in the friction coefficient by more than 30% and an improvement in the lubrication effect, thus prolonging the service life of artificial hip joints. Qin et al. [71] initiated the development of pure inorganic graphene oxide/water dual-responsive hydrogels. Through pH/temperature-triggered microstructure reconfiguration, the friction coefficient was dynamically regulated, showing a five-fold decrease at low pH, mimicking the adaptive behavior of biological tissues during tribological processes. Zhang et al. [72] fabricated conductive hydrogel films using the film casting method and glycerol–water secondary hydration. This ultrathin-structured hydrogel exhibited a fracture elongation rate as high as 523.3%, a stress of 3.5 MPa, and good friction resistance. Moreover, it endowed the sensor with excellent sensing performance (a gauge factor of 2.1 and a response time of 170 ms). Hu et al. [73] put forward a polyvinyl alcohol/chitosan hydrogel featuring a dual physical crosslinking network fabricated through multiple processing techniques. Under aqueous conditions with a load of 30 N and a frequency of 1 Hz, the friction coefficient of the hydrogel was around 0.05. Moreover, it exhibited remarkable long-term lubrication performance throughout 100,000 reciprocating cycles, without suffering from destructive wear or structural dete-

rioration. Lee et al. [74] explored a dual-network hydrogel, where the first network was formed by physically crosslinked agarose, and the second network consisted of a chemically crosslinked acrylamide/acrylic acid copolymer. Their findings indicated that friction stemmed from the shear of the polymer network. Additionally, at higher sliding velocities, the augmentation of fluid dynamics and viscoelastic deformation became more prominent. He et al. [75] designed targeted hydrogel microspheres for the precise lubrication of local cartilage lesions in bone joints. In comparison with hyaluronic acid, the friction coefficient of this hydrogel decreased by 35.5%, offering a novel strategy for the early intervention of osteoarthritis.

In recent years, investigations into hydrogels have augmented their mechanical resilience and environmental adaptability. The majority of hydrogels are prone to losing their lubricating layer under conditions of high shear and cyclic loading. This phenomenon results in a deterioration of their overall performance when they are removed from the biomimetic environment. At elevated temperatures (above 60 °C) or low temperatures (below −20 °C), the network structure of hydrogels becomes unstable. This instability causes the hydration layer to rupture, thereby resulting in a sudden surge in the friction coefficient. Furthermore, there is a dearth of dynamic multi-parameter coupling testing platforms that can accurately mimic the biological environment. Consequently, in the future, through the design of intelligent responsive materials, the innovation of self-repair mechanisms, the synergy of green and high-toughness properties, and the integration of medical and engineering applications, it will be feasible to achieve on-demand switching of friction performance. This approach will offer solutions for high-risk scenarios and personalized biomimetic material replacements.

2.1.3. Green Lubricants Based on Nano-Lubricants

- MoS_2

The lubricity of MoS_2 is ascribed to its layered hexagonal crystal structure. The layers are bound by weak van der Waals forces, giving rise to a low sliding barrier and an extremely low coefficient of friction (which can be as low as 0.01). Studies reveal that its lubrication behavior can be classified into two approaches. The first lubrication approach is intragranular slip [76,77]. In the atmospheric environment, MoS_2 forms an ordered transfer film through self-oriented arrangement, minimizing the direct contact of the friction pair and significantly reducing the wear rate [78]. The second lubrication approach is rolling motion [79,80]. Under vacuum or high shear stress conditions, MoS_2 nanosheets can be wound to form "nanospheres", further lowering the coefficient of friction through a rolling friction mechanism, particularly demonstrating outstanding lubrication life in a vacuum environment [81]. Additionally, the heterojunctions formed by MoS_2 and materials such as graphene, due to lattice non-commensurability (structural mismatch) [82–85], can decrease the interlayer slip potential barrier and enhance the cooperative lubrication performance. MoS_2 displays irreplaceable lubricating advantages under extreme conditions such as high temperature (~1200 °C), low temperature (~−190 °C), high vacuum, and high load. Yang et al. [86] developed a multifunctional magnetic lubrication system, MoS_2@STAX, via the electrostatic self-assembly method and discovered that dense carbon layers and oxide films formed between the interfaces at high temperatures, which significantly reduced friction and wear. Li et al. [87] grafted MoS_2 and incorporated it into the perfluoropolyether lubricant, reducing the friction coefficient of the lubricating oil by 36.8% at 250 °C. Long et al. [88] found that the MoS_2/graphene heterojunction could still maintain ultra-low friction at a high temperature of 850 K. Our research group [89] previously investigated the lubrication performance of MoS_2 under ultra-low temperature conditions (20 K) and heavy loads (>1 GPa), with a friction coefficient as low as 0.0001 and nearly zero wear. Liu et al. [90]

prepared Ni-MoS_2/graphite coatings by supersonic atmospheric plasma spraying and achieved low wear under a heavy load of 15 N, with a wear rate of 2.21 × 10^{-4} mm^3/N·m. MoS_2 coatings are employed in engine components and space machinery. Their ultra-low friction properties in a vacuum environment can prolong the service life of equipment and mitigate safety risks resulting from lubrication failure. Serles et al. [91] fabricated a novel type of MoS_2/TaS_2 coating, which can be utilized in the ground and ultra-high vacuum (10^{-6} Pa), and it represents the first all-purpose space lubricant with high performance in both terrestrial and deep space environments. Song et al. [92] carried out a study on the bimodal and contact modes of MoS_2 and Au using ultra-high vacuum atomic force microscopy, demonstrating that the rigid friction coefficient of the MoS_2 surface crossing a single Au (111) step is extremely low, opening up a new minimization approach for nanoscale electronic devices utilized in aerospace lubrication. Moreover, Guo et al. [93] discovered through molecular dynamics (MD) research that a MoS_2 surface-modified with oleic acid can be adsorbed onto the metal surface and form a stable boundary lubricating film under high pressure.

Despite MoS_2 exhibiting excellent tribological properties in high-temperature, low-temperature, and vacuum environments, under high-load or impact conditions, the coating experiences crack propagation. This is attributed to the shear layer failure mechanism and its brittle nature, leading to interlayer slip failure or surface spalling, thereby failing to meet the requirements of heavy-duty mechanical systems. Moreover, MoS_2 is highly vulnerable to humidity and oxygen, which results in augmented wear. Babuska et al. [94] successfully converted atomic layer-deposited MoO_x into MoS_2 through annealing in a hydrogen sulfide atmosphere at temperatures ranging from 200 to 550 °C. This process led to the formation of a highly ordered basal plane-oriented surface microstructure. The resulting atomic layer-deposited MoS_2 coating can serve as a green solid lubricant for low-temperature operations in aerospace applications. Behrens et al. [95] fabricated single molybdenum and single molybdenum trioxide coatings via physical vapor deposition (PVD). Then, they developed a wear model grounded on the friction coefficient and corroborated the environmental advantages of the Mo/MoO_3 composite solid lubrication system through reverse verification by means of wear experiments. Rodríguez Ripoll et al. [96] were the first to report the in situ sulfidation of MoO_3 nanotubes during sliding contact in the presence of sulfur-containing lubricant additives. This phenomenon gave rise to the formation of a low-friction tribochemical film enriched with molybdenum disulfide. Michalczewski et al. [97] discovered a highly positive synergistic effect between traditional anti-wear additives and MoO_3 as well as MoS_2 nanotubes. These materials demonstrated excellent tribological properties at 200 °C. Furthermore, the preparation of MoS_2 coatings depends on vacuum technologies such as PVD or chemical vapor deposition. Precise control of the process parameters, including the temperature and deposition rate, is essential. Even slight deviations can significantly impact the tribological properties, resulting in elevated production costs and challenges in large-scale production. Consequently, in the future, multidisciplinary mechanism research and technology integration should be conducted to enhance its hydrophobicity and optimize the coating preparation processes. This approach aims to strike a balance between tribological performance requirements and environmental adaptability.

- Graphene

With zero heavy metal content and chemical inertness, graphene adheres to the tenets of green chemistry and is well-suited for the lubrication of precision instruments. Recent key progress has broken through the bottleneck of dispersion stability [98–100]. Marchetto [101] and Shi [102] et al. discovered that under vacuum conditions, the friction coefficient of few-layer graphene can reach as low as 0.02, far exceeding that of soft metal materials

(friction coefficient ~0.2). The lubrication mechanism lies in the fact that the weak van der Waals forces between layers facilitate interface sliding and suppress adhesive wear. Notably, in a vacuum environment, although the friction coefficient of multi-layer graphene is slightly higher than that of few-layer graphene, it can still be as low as 0.05 [103,104]. This is because the layers of multi-layer graphene are coupled by van der Waals forces. During the sliding process, it is necessary to overcome the cumulative shear resistance of multiple interfaces, leading to the superposition of shear stress. Moreover, under load, interlayer elastic deformation is likely to occur, forming local wrinkles and increasing energy dissipation. Pape et al. [105] found that in a dry environment, graphene sheets would form a dense transfer film on the contact surface of steel balls. The research team led by Professor Zhu from Southwest Jiaotong University [106–108] successfully achieved high-density dispersion of graphene in lubricating oil (i.e., without sedimentation or layering) through surface organic group modification and atomic hybridization technology. This accomplishment effectively addressed the issue of lubrication failure caused by the π-π aggregation of traditional graphene. Functionalized graphene additives incorporated into gear oil have demonstrated the ability to effectively reduce contact stress, suppress bidirectional friction fatigue, and extend the lifespan of components by over 30%. These additives have been successfully applied in hydraulic systems and high-speed rail bearings [109]. When compounded with MoS_2, the anti-friction and anti-wear properties of the resulting material are enhanced by 13.0% and 37.4%, respectively. Solid–liquid synergistic lubrication can efficiently address friction and wear issues through the combined action of solid and liquid lubricants. Shi et al. [110] fabricated a Cu composite coating consisting of W particles and lubricating graphene nanoplatelets (GNPs) via cold spraying technology. Their findings revealed that the Cu-W-GNPs coating exhibited an extremely low friction coefficient of 0.16 and wear rate of 1.9×10^{-5} $mm^3/N{\cdot}m$. Ye et al. [111] appropriately introduced few-layer graphene as a reinforcing material into the high-entropy alloy CoCrFeNiMn using the protocol model alloy approach. This addition led to a reduction in the wear rate and friction coefficient by 86.03% and 23.87%, respectively, simultaneously achieving both lubrication and surface strengthening. Zheng et al. [112] Investigated the tribological behavior of epoxy/graphene composites by varying the lubrication conditions. Their research showed that the dry friction coefficient of the composite material was decreased by 27.3%, and the lowest friction coefficient in oil amine was 0.0389.

Despite the verification of graphene's salt fog corrosion resistance and environmentally friendly characteristics in aircraft, high-speed rail, and marine applications, several bottlenecks remain to be addressed for its utilization as a green lubricant. Firstly, the functionalization modification of graphene necessitates precise control over the number of layers and surface groups. This requirement restricts its scalability and process compatibility. Secondly, under extreme conditions, the long-term effectiveness of graphene is inadequate. At high temperatures, the graphene layers are susceptible to oxidative delamination, leading to the rupture of the lubrication film. At low temperatures, its dispersion stability is diminished. Finally, the friction chemical evolution pathway of graphene in multi-field coupling environments, such as those involving heat, force, and electricity, remains unclear. In the face of these challenges, by integrating graphene with hydrogel, the lubrication behavior can be adjusted via pH/temperature triggers, thereby expanding into the realm of adaptive precision transmission. Additionally, it is feasible to reduce costs and achieve recyclability by enhancing the hydrophobicity of graphene. Moreover, graphene-based lubricating grease can concurrently resolve the issues of electro-corrosion and wear and find application in the remanufacturing of mining machinery.

- Silver

At elevated temperatures, the low shear (111) crystal plane of silver experiences lattice slip, thereby forming a self-repairing silver lubrication film [113–115]. Silver ions can confer antibacterial functions through a slow-release mechanism (0.5–5 ppm), thereby preventing the generation of environmental pollutants and fulfilling the green lubrication requirements of high-end equipment, such as aircraft engines. Taha-Tijerina et al. [116] Conducted an assessment of the thermal transfer behavior of biodegradable lubricants incorporated with silver nanostructures. Their findings indicated that under isothermal conditions, the decomposition time was prolonged. de Castilho et al. [117] fabricated silver-containing coatings via thermal spraying. It was observed that, at 350 °C, the friction was significantly diminished, and smooth multi-layer transfer films were formed on the contact surface. Jackson et al. [118] utilized silver nanoparticles to enhance the performance of dodecane lubricants. They discovered that silver could decrease and stabilize the contact resistance, as well as mitigate the friction and wear. Hu et al. [119] carried out tribological evaluations of lubricating oils containing silver precursors at room temperature and 300 °C. The results showed that in both scenarios, the friction coefficient was reduced, leading to mild wear. Twist et al. [120] reported a novel silver pyrazole–pyridine complex and demonstrated that it could improve the friction and wear performance of engine oil at elevated temperatures. Shi et al. [121] conducted an in-depth investigation into silver-containing TiAl-based self-lubricating composites. Their findings revealed that within the temperature range of 25 °C to 800 °C, the friction coefficient of these composites was lower than that of the matrix alloy. Zhu et al. [122] made a significant discovery regarding Ni_3Al-based composites with the addition of silver and V_2O_5. They reported that from room temperature to 1000 °C, the friction coefficient of these composites ranged from 0.25 to 0.4, and the wear rate at high temperatures was approximately 10^{-5} mm^3/Nm. The achievement of lubrication over a broad temperature range was attributed to silver and the in situ formed silver vanadate lubrication at elevated temperatures. Tyagi et al. [123] fabricated nickel-based composites incorporating silver nanoparticles and boron nitride nanoparticles via powder metallurgy. Through ring-on-block tribological tests, it was observed that the friction coefficient decreased as the temperature increased. Wan et al. [124] synthesized solid organic lubricating coatings filled with silver nanoparticles in situ. Their research demonstrated that both the friction coefficient and wear rate were significantly reduced, and the lubrication effect of RP-3 aviation kerosene was also enhanced.

Nanosilver exhibits a propensity for agglomeration and has a tendency to sediment, when it is stored in lubricating oil over an extended period. To improve its stability, the addition of composite stabilizers becomes essential. However, this not only increases the complexity of the process but may also exert an impact on the mechanical properties of the material and its long-term biocompatibility. In medical applications, the cytotoxicity of nanosilver remains incompletely understood. Furthermore, although environmentally friendly processes such as supercritical CO_2 technology are available, they demand substantial equipment investment and elevate production costs. In the future, leveraging the synergistic effect of composite materials can enable the creation of a dual-mechanism lubrication system featuring "physical isolation + chemical transfer film". This would serve to increase the thickness of the oil film and reduce the wear rate. Additionally, a nanosilver crystal structure layer can be formed through current-carrying friction, thereby stabilizing the contact resistance and offering a high wear resistance and low impedance solution for electrical contacts in new energy vehicles. Even though the industrialization of nanosilver green lubricants still needs to address challenges such as environmental toxicity assessment and recycling design, their performance advantages in high-end equipment, biomedicine, and new energy sectors will continue to drive the innovation of green tribological materials.

2.2. Wear Mechanisms of Green Lubricants

Green lubricants are typically added as raw materials or fillers for processing and production, resulting in wear that influences the processing procedure and quality. The four widely acknowledged mechanisms of wear in the academic field are adhesive wear, abrasive wear, fatigue wear, and corrosive wear [125]. Investigating the friction behavior and wear mechanisms between green lubricants and the body surface poses a challenge. When investigating the material movement, friction behavior, and wear mechanism of green lubricants, a combination of friction and wear experiments and discrete element numerical simulation can be employed to study the tribological properties of the tribology system.

Previous studies have probed into the wear mechanisms between solid particles and mechanical surfaces. Li et al. [126] employed a combination of experiments and simulations to study the performance and wear mechanisms of the spiral blades of pavers through impact, pin-on-disk, erosion wear tests, and wear morphology analysis, discovering that systems with a base of high-chromium alloy steel and coatings of silicon carbide and tungsten carbide particles exhibit the best wear resistance; they further calculated the wear failure modes of the spiral blades using EDEM software, finding that the wear amount escalated from the spiral shaft to the outer edge of the spiral blade. Hoormazdi et al. [127] employed a combination of experiments and simulations to study the performance and wear mechanisms of the spiral blades of pavers through impact, pin-on-disk, erosion wear tests, and wear morphology analysis, discovering that systems with a base of high-chromium alloy steel and coatings of silicon carbide and tungsten carbide particles exhibit the best wear resistance. They further calculated the wear failure modes of the spiral blades using EDEM software, finding that the wear amount escalates from the spiral shaft to the outer edge of the spiral blade [128], computed the material removal quantity during the precision machining of main spindle drums based on Hertz–Mindlin and Archard Wear theories in EDEM, and analyzed the machining mechanism in light of the particle trajectories and corresponding contact forces obtained from simulations and experiments. Han et al. [129] investigated the wear mechanism of carbon black particles on rotors of internal mixers through a combination of experiments and EDEM simulations. The wear mechanisms of the green lubricants are summarized in Table 1.

Table 1. The wear mechanisms of green lubricants.

Green Lubricants	Structural Features	Wear Mechanisms
Cellulose	The hydroxyl groups (-OH) on the molecular chain form a physical adsorption film with low shear strength on the surface of the friction pair.	The fracture and spalling of molecular chains occur under the action of shear force. Under long-term high loads, abrasive wear may be induced due to the rupture of the film.
Vegetable oil	The polar carboxyl groups (-COOH) chemically adsorb onto the metal surface, thereby forming a compact monomolecular boundary film.	The periodic rupture and regeneration of the adsorption film (mild adhesive wear) may occur. At elevated temperatures, oxidation products can induce corrosion wear or abrasive wear resulting from carbon deposition.

Table 1. *Cont.*

Green Lubricants	Structural Features	Wear Mechanisms
Ionic liquid	Cations (e.g., imidazolium and pyrrolidinium) are adsorbed onto the surface of negatively charged metals via electrostatic interactions. Anions (e.g., $[BF_4]^-$ and $[TFSI]^-$) form a double-layer barrier with low shear resistance.	Under high contact pressures, chemical reaction films containing fluorine, phosphorus, and boron elements are formed. The dominant phenomenon is the slight spalling of the reaction films, which effectively suppresses adhesive and fatigue wear.
Hydrogel	Hydrodynamic lubrication is dominant. The three-dimensional network structure releases a substantial amount of bound water under high loads, thereby forming micro-scale water films.	Fatigue fracture resulting from the cyclic elastic deformation of the network structure or adhesive wear caused by local dehydration; nevertheless, the self-healing characteristics can partially repair frictional damage.
MoS_2	Low-shear slip, which is induced by the weak interlayer van der Waals forces, causes the S-Mo-S interlayer structure to undergo directional alignment. As a result, a transfer film is formed to cover the surfaces of the friction pair.	The high load-bearing capacity and the stress dissipation characteristics of the layered structure contribute to an enhanced anti-wear capacity. The dominant wear mechanism is the progressive spalling (lamellar dissociation) of the transfer film. Additionally, the formation of MoO_3 due to high-temperature oxidation can induce abrasive wear.
Graphene	An ultrathin shear layer is established between the friction pairs via physical adsorption. The π-π stacking within the layer gives rise to an extremely low shear resistance.	The anti-wear performance can be improved by sp^2-hybridized carbon networks and self-repair of defects. Progressive exfoliation resulting from the interlayer slip, along with edge oxidation, may induce extremely high local abrasive wear.
Silver	Silver nanoparticles form a ductile transfer film on the surface of the friction pair via a diffusion mechanism.	The high thermal conductivity of silver (which mitigates local temperature increases) and its re-passivation capacity contribute to an improvement in the anti-wear performance. Under cyclic loading conditions, fatigue spalling is the dominant failure mode of the transfer film.

The simulation results demonstrated the heavily worn areas on the rotor, revealing that the degree of rotor wear is proportional to the speed and filling ratio, and the simulation results were confirmed by the experimental results.

3. The Current Status of EDEM

Considering the distinctive complexity of the tribological properties of green lubricants (including bio-based lubricants, water-based lubricants, nano-lubricants, and systems

incorporating environmentally friendly additives), the friction coefficient, wear rate, and load-carrying capacity are not merely significantly affected by the physical and chemical characteristics of the base material and environmental factors (such as the temperature, humidity, and vacuum level) but also intricately associated with their core mechanisms at the microscale. Representative mechanisms encompass the formation and breakdown of boundary lubrication films, microscopic contact, and material transfer, as well as particle-mediated wear and lubrication. To conduct a thorough analysis of the friction process at both macroscopic and microscopic scales, particularly the dynamic behavior at the particle scale and its cross-scale influence on macroscopic tribological properties, traditional continuum mechanics models and macroscopic experimental characterizations frequently prove insufficient. At present, the discrete element method (DEM), a potent particle dynamics simulation technique, has manifested its distinctive value and robust continuity. It is capable of visualizing and quantifying microscopic mechanisms, simulating boundary film formation and additive effects, replicating particle-mediated wear processes, and conducting parameter sensitivity studies and optimization. Consequently, DEM simulation technology offers a powerful computational experimental approach for a deeper understanding of the physicochemical essence underlying the intricate tribological properties of green lubricants, particularly the pivotal role of particle-scale dynamics. It effectively fills the cognitive gap between the macroscopic performance characterization and the microscopic action mechanism of green lubricants. As an essential research tool, it is crucial for uncovering their friction, wear, and lubrication laws, ultimately attaining the objectives of high performance and extended service life. The simulation results of DEM can not only account for experimental phenomena but also forecast performance under novel formulations or extreme conditions, significantly expediting the research and development process of green lubrication technology.

DEM originated from molecular dynamics. In the 1970s, Cundall and Strack were the first to propose the concept of DEM [130,131]. In 1980, Cundall developed the UDEC program [132]. In 1984, Lorig devised a novel coupling method to overcome previous computational deficiencies [133]. Before the 1990s, research on discrete element methods mainly centered on two-dimensional aspects. By the 1990s, the ITASCA company in the United States developed PFC2D/3D discrete element simulation software based on the discrete element method [130]. In the 21st century, DEM Solutions, UK, developed EDEM [134–136], which is the world's first general-purpose computer-aided engineering (CAE) software designed for simulating and analyzing particle handling and production operations using modern discrete element modeling technology. It employs DEM technology to enhance the computing function, enabling rapid and precise simulation and analysis of the behavior of solid particles such as ores, fibers, and powders in diverse application scenarios. Currently, it is extensively utilized in industries like aerospace, chemical engineering, agriculture, and mining. Foreign-developed discrete element simulation software mainly comprises the EDEM, Universal Discrete Element Method Program (UDEC), 2D/3D Particle Contact Dynamics Finite Element Program (PFC2D/3D), and 3D Discrete Element Method Program (3DEC).

Research on the discrete element method in China began relatively late, as depicted in Table 2. In 1986, Professor Wang Yongjia and Professor Wan Xi from Northeastern University introduced the principles of the discrete element method to China [137]. In 2014, a domestic company released the first discrete element method software, StreamDEM. In 2019, at the 15th China CAE Engineering Analysis Technology Annual Conference, the discrete element method software MatDEM developed by Nanjing University was awarded the "China Digital Simulation Autonomous Software Innovation Award". Nevertheless, in contrast to foreign software, the application rate of domestically produced discrete

element software is relatively low, and there remains a considerable gap in performance, functionality, etc., when compared with foreign software. The domestically developed discrete element simulation software mainly encompasses Matrix Discrete Element MatDEM, StreamDEM, 2D-Block Discrete Element Analysis System, TRUDEC, and SuperDEM. They are employed for simulations such as particle grinding, material transportation, particle crushing, etc., to investigate the interactions and motion states between discrete solid materials and the matrix. Gui et al. [138] employed UDEC and a mixed-mode cohesive fracture model to numerically simulate the drying cracking of laboratory soil. Wang et al. [139] utilized MatDEM particle flow software to investigate the mechanical response characteristics of fractured sandstone under different principal stresses in true triaxial conditions, exploring the mechanical response characteristics, fracture mechanisms, and damage evolution characteristics of sandstone specimens under three distinct pressure conditions, thereby verifying the rationality of particle flow simulation experiments.

Table 2. The process of development of the EDEM.

Year	Key Achievements
1970s	The concept of the discrete element method was first proposed [131]
1980	Application of UDEC [132,140]
1986	The principle of the discrete element method was introduced for the first time in China [137]
1990s	The USA developed PFC2D/3D discrete element simulation software [138,141]
2000s	The UK developed EDEM software [134]
2014	China developed StreamDEM software [142,143]
2019	The MatDEM software developed in China won the award [139]
2025	CPU acceleration, multi-physics field coupling capability, material model, and contact mechanism [144–146]

To date, EDEM has witnessed leapfrog advancements in three domains: computing architecture, multi-disciplinary coupling, and industrial applications [147–149]. Its core strength lies in resolving engineering issues of complex particle systems via high-precision simulation. However, in the realm of green lubricant research, accurately capturing the microscopic interactions (such as van der Waals forces, electrostatic effects, and surface energy effects) of nano-additives (e.g., hexagonal boron nitride nanosheets) remains a challenge for traditional contact models. Concurrently, EDEM simulation hinges on precise contact model parameters (including friction coefficient, surface energy, and adhesion). Nevertheless, calibrating the interface characteristics of green lubricants demands a substantial amount of experimental evidence, and functionalization further exacerbates the uncertainty of the model parameters. Moreover, given the complexity of environmental working condition parameters, EDEM's simulation capabilities for solid–liquid–gas multiphase interfaces and thermal–mechanical–chemical coupling are constrained. Looking ahead, enhancing computing efficiency through GPU and multiphysics acceleration, along with algorithmic innovation, will render it an essential tool in domains such as machinery. Simultaneously, with the deeper integration of artificial intelligence and high-performance computing, the latent potential of EDEM in real-time simulation and intelligent design optimization can be further explored.

By computing the motion of each unit cell, EDEM is capable of depicting the movement of granular materials in channels, predicting the overall movement of the research object, and is currently extensively utilized in engineering for discrete element simulations, especially for investigating the wear between discrete materials and mechanical components. Chen et al. [150] employed EDEM software to predict the sliding wear mechanism

of iron ore particles, providing data support for enhancing the wear resistance of equipment transporting iron ore. Li et al. [126] utilized EDEM software to construct a paver model, studying the wear of different materials of spiral blades and finding that samples with a wear-resistant coating of titanium carbide/tungsten carbide (TiC/WC) particles exhibited the best wear resistance. Liu et al. [151] investigated the wear of drum blades of thin coal seam mining machines via simulation analysis, establishing coupling models of diverse drum speeds, different blade helix angles, and various gangue hardness coefficients. Yang et al. [152] constructed a novel spiral blade wear model based on the Archard wear model and the continuum hypothesis, validating wear patterns through EDEM simulation to predict the lifespan of spiral blades. Our research group also achieved initial progress in experimental and simulation studies [153,154] of cross-viscosity cellulose on wear surfaces. Through EDEM simulation, it was discovered that as the viscosity of cellulose rose, the contact area between cellulose and the surface decreased, reducing the relative sliding of cellulose in the groove and thereby reducing wear in the groove. Additionally, the primary factor influencing cellulose wear is the load, with wear significantly escalating as the load increases.

4. Friction and Wear Experiments with Green Lubricants

The tribological properties of green lubricants, including time-varying friction coefficient curves, wear rates, extreme loads, and anti-sintering capabilities, need to be quantitatively characterized using standardized friction and wear testing apparatuses. Testing machines, such as four-ball testers, ring-on-block testers, high-frequency reciprocating testers, and fretting wear testers, can replicate the service scenarios of real friction pairs (e.g., ball-on-disc and face-to-face contacts) at the laboratory scale. This is achieved by accurately controlling the operating parameters, such as the normal load, sliding speed, temperature, and contact form, as well as the environmental media, including the humidity and oxygen content. The macroscopic performance data output by these machines, such as the average friction coefficient, wear scar diameter, and wear volume, serve as direct evidence for evaluating the applicability of lubricants. Nevertheless, the macroscopic data obtained from the testing machines are insufficient to uncover the microscopic origins of the performance discrepancies in green lubricants. At this juncture, the discrete element method (DEM) functions as a crucial bridge that links macroscopic experiments with microscopic mechanisms. Specifically, leveraging the macroscopic boundary conditions (such as the load, speed, and temperature field) measured by the testing machine, DEM is capable of constructing a virtual friction pair that is consistent with the experimental geometry. By incorporating real surface topography data obtained from techniques like white light interferometry or atomic force microscopy and precisely defining the particle-level forces (including the van der Waals force, liquid bridge force, and cutting force), DEM enables high spatiotemporal resolution analysis of microscopic processes.

The integration of DEM and the friction and wear testing machine gives rise to a "virtual–experimental" closed-loop research paradigm. In this paradigm, experiments serve as the driving force for DEM modeling, while DEM offers in-depth explanations for experimental phenomena. Subsequently, a further joint optimization design is implemented. The friction and wear testing machine provides essential performance benchmarks, and DEM uncovers the underlying action mechanisms. Collaboratively, these two approaches contribute significantly to the advancement of green lubricants. Friction and wear testing machines are machines that use microcomputer control, dynamic display on a monitor, and electromechanical integration principles to conduct friction and wear tests under certain conditions. They are used to study the tribological properties and wear mechanisms of materials. There are many types of friction and wear testing machines, and according to the

statistics, there are currently more than 200 types [155]. The motion forms of the friction pair in the friction and wear testing machine are shown in Figure 2.

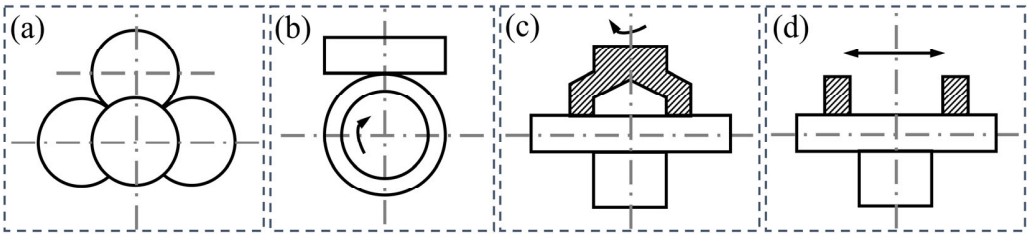


Figure 2. The motion patterns of the friction pair in the friction and wear testing machine. (**a**) Fourball, (**b**) ring-block, (**c**) face, and (**d**) face-to-face.

4.1. Commercial Friction and Wear Testing Machines

The research on friction and wear testing machines began in the early 20th century. The first abrasive wear testing machine was created in 1910 [156]. In the initial stages, the design of testing machines was rather simple, mainly simulating the friction and wear process manually or mechanically. In 1930, a four-ball friction tester was first fabricated by the Shell company. In 1965, a four-ball friction tester appeared in China at the Jinan Experimental Machine Factory [155]. By 1975, there were already hundreds of diverse types of friction and wear testing machines known [157], mainly applicable for tests at room temperature. In the early 1980s, Soemantri et al. [158], in the United States, commenced researching high-temperature wear testing machines and jointly developed three high-temperature abrasive wear testing machines. By the late 1980s, Fischer et al. [159], in Germany, developed a controllable atmosphere three-body high-temperature wear testing machine. In the 21st century, the RTEC Company, in the United States, developed a multifunctional friction and wear testing machine to broaden the testing conditions of the same machine based on CETR Olympus [160], thereby diversifying the testing functions. Supported by computer technology, software programming technology, microelectronics technology, and signal communication technology, the friction and wear testing machine has now evolved to simulate various working conditions such as high speed, low speed, heavy load, light load, dynamic changes, and various environmental conditions such as high temperature, low temperature, vacuum, inert gas, radiation, etc. [161], and to meet the requirements of continuous automatic testing, high accuracy of electrical measurement and control systems, good stability, and ease of operation. Domestic and international universal friction and wear testing machines encompass four-ball testing machines, Optimol SRV® testing machines, CMS testing machines, Falex testing machines, Timken testing machines, UMT multi-functional friction and wear testing machines, LFW-1 testing machines, MM-1000 friction and wear testing machines, etc. [155]. The principal manufacturers of friction and wear testing machines are Optimol GmbH in München, Germany, Falex Corporation in Sugar Grove, IL, USA, Brooks Corporation in Seattle, WA, USA, CMS Tribotechnologies in Geneva, Switzerland, Tokyo Kogyo Corporation in Tokyo, Japan, and Jinan Testing Machine Manufacturing Corporation in Jinan, China and Shanghai Instrumentation Co., Ltd. in Shanghai, China [155]. Currently, there remains a considerable disparity in performance, accuracy, and other aspects when comparing testing machines.

4.2. Self-Built Friction and Wear Testing Machine

In addition to enterprises engaged in the development and production of friction and wear testing machines, numerous research institutions and universities are independently undertaking research and development on the design of friction and wear testing machines. The Lanzhou Institute of Chemical Physics of the Chinese Academy of Sciences [162]

has fabricated an HT-500 type friction and wear testing machine that can operate up to 100 °C, enabling tests on diverse friction pairs such as pin-disc or ball-disc in high-temperature environments and inert gas atmospheres like nitrogen, carbon dioxide, and helium. Duranty et al. [163], from the Northwest Pacific National Laboratory in the United States, have investigated an in situ friction testing machine for measuring polymer friction and wear in high-pressure hydrogen environments, with a pressure reaching 3800 psi, offering equipment support for exploring the influence of high-pressure hydrogen on polymer friction and wear. Zhang et al. [164] have developed an ultra-high-speed ball-disc testing machine with a maximum reciprocating sliding speed of 50 m/s, offering a broad speed range and high versatility in practice.

In addition to the common environmental friction and wear testing machine, there are also friction and wear testing devices for special environments. Ma et al. [165] is capable of testing in a vacuum environment with a maximum ultimate pressure of 6×10^{-6} Pa, attaining a high vacuum state in a short period and featuring high testing efficiency. Francis et al. [166] have devised and fabricated a disc-type friction testing machine capable of conducting low-temperature friction and wear tests under liquid nitrogen (wet test) or dry sliding circumstances. Zhang et al. [167] have developed a shaft-sleeve type friction and wear testing machine featuring a controllable atmosphere environment, which can be employed to investigate the friction and wear regulations of friction pairs in air and nitrogen atmospheres. Cheng et al. [168] have constructed a multifunctional environment-controllable friction and wear testing machine, which can dynamically adjust the humidity and temperature by modifying the control modules and can carry out reciprocating and rotating motions, attaining the function of multi-purpose utilization with one machine. Our research group has also established a small surface-to-surface friction and wear testing machine [154,169], achieving a maximum load of 25 N and adjustable rotational speed through a pneumatic control system (Figure 3). The structure of the face-to-face rotating friction and wear testing machine mainly consists of a frame, motor, upper friction pair, lower friction pair, cantilever rod, cantilever beam-type force sensor, standard weights, loading platform, sliding guide mechanism, etc.

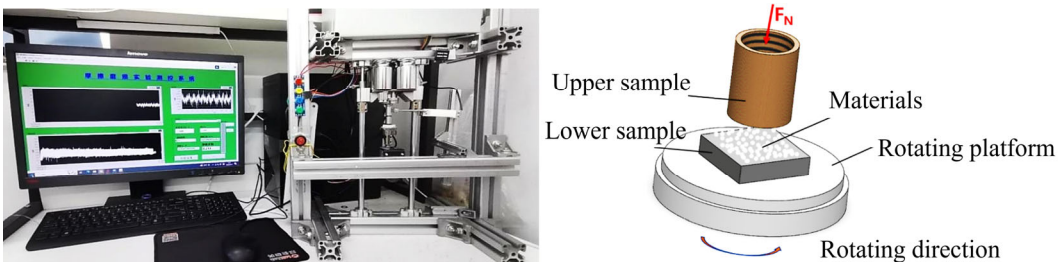


Figure 3. Face-to-face rotating friction and wear testing machine.

4.3. Intelligentization of the Friction and Wear Testing Machines

Friction and wear phenomena entail multi-scale interfacial interactions. Traditional experimental approaches encounter challenges in capturing dynamic changes in real time. The integration of intelligence into friction and wear testing machines can significantly enhance the precision of analyzing crucial parameters, such as the coefficient of friction and the film thickness ratio, through the utilization of sensor networks and machine learning models. When high-end equipment operates under extreme conditions, including high temperature, high load, and high speed, it invariably results in accelerated wear of friction pairs and augmented energy consumption. Leveraging the real-time monitoring and dynamic control capabilities of intelligent testing machines, the performance matching degree of green lubricants can be optimized, thereby extending the service life of the equipment.

Furthermore, the intelligent friction and wear testing machine can effectively verify the long-term stability and environmental adaptability of green lubricants via multi-physical field coupling simulations. This not only streamlines the experimental process but also reduces the costs associated with experimental iteration. With the progress of microelectronics technology, semiconductor ultra-large-scale integrated devices, particularly the maturity of microelectronic computer technology, the development of electrical measurement and control systems is constantly moving towards intelligentization [170]. The characteristics of the electrical measurement and control system of the friction and wear testing machine mainly involve the research on new sensors and high-performance motor systems [171]. Friction and wear testing machines capable of simulating more complex working conditions have been developed. The design of the electrical measurement and control system holds a crucial position in determining the operability, stability, experimental accuracy, and other performance aspects of the friction and wear testing machine. Currently, the utilization of computer-assisted technology for the development of friction and wear testing machines represents a major trend. By employing computer control technology, the machines can automatically accomplish various operations by logical programs, and the data acquisition system is designed in the form of "sensor-signal conditioning-data—data acquisition card–software" [172]. A complete measurement and control system is typically divided into signal flow processes, including signal acquisition (sensors), signal conditioning, signal processing, signal display, and transmission, along with AC/DC power supplies and control circuits, thereby forming a complete system structure as shown in Figure 4. According to the diagram, sensors and various instruments used for collecting sensor signals, as well as diverse hardware for data display and recording, deal with the input and output of signals. Nevertheless, signal processing constitutes the core of the measurement and control system, and the software employed for signal processing is of crucial significance in determining the overall performance of the system.

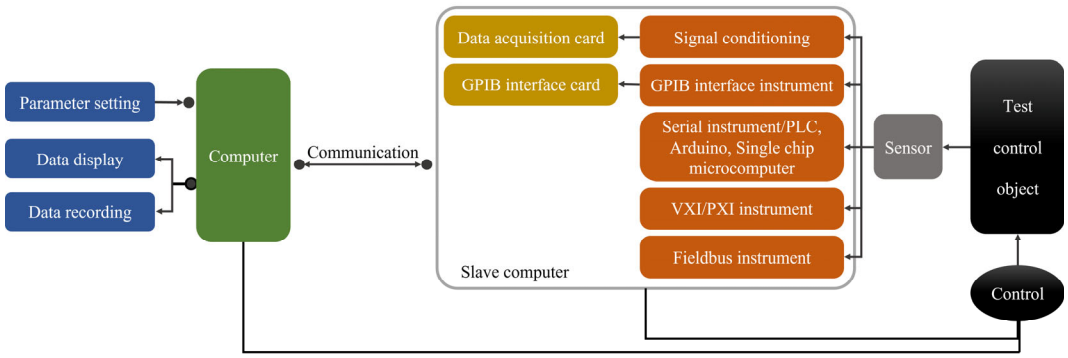


Figure 4. Schematic diagram of the control system for the friction and wear testing machine.

The computer, in combination with various interface devices, forms a comprehensive electrical measurement and control system. The core of this system is the computer, which governs and processes data for the entire system. Its main function is to act as a host for signal processing, display, and the issuance of control commands. Host computer software is often developed by using text-based programming languages such as Visual C, Visual Basic, and Lab Windows/CVI, as well as graphic programming software like LabVIEW, ArduinoIDE, and KingView. Various interface devices include data acquisition cards, GPIB interface cards, serial instruments, VXI/PXI instruments, and field bus devices. Through the integration of host computer software and various interface devices, it becomes feasible to collect sensor data and control conditions such as the motor speed, temperature, humidity, and load. In the design process, a hierarchical structure like Chai's [173] computer and programmable logic controller (PLC) coordination is frequently employed. This allows the

computer to issue control commands to the PLC, which then governs the servo motor. The PLC collects sensor data and transmits them to the computer for data processing and display. There are numerous design schemes for the electrical measurement and control system of friction and wear testing machines, with manufacturers and scholars worldwide conducting relevant research and achieving design results. Since the host computer software constitutes the core of the measurement and control system, it is classified based on the development platform utilized for the computer software. The intelligence of friction and wear equipment has been remarkably improved, enabling enhanced repeatability and accuracy in green lubricant research. This is achieved through multi-parameter dynamic regulation, cross-scale simulation, and real-time feedback mechanisms. By integrating multi-scale simulation techniques, such as the coupling of EDEM and MD, it becomes possible to precisely capture the interface behaviors of green lubricant particles, including interlayer slip and electron distribution. Moreover, in situ monitoring technology can be employed. Through the friction electrical signal feedback system, the interface state of the friction pair surface, such as the film thickness and pressure distribution, can be quantitatively analyzed in real time. Looking ahead, it is essential to further incorporate the friction chemical mechanism and AI algorithms to construct a full-chain intelligent platform encompassing "material design—performance verification—service monitoring". This will facilitate the transition of green lubrication technology from laboratory settings to engineering applications.

5. Conclusions and Prospects

This paper incorporates the pertinent research that integrates numerical simulation and friction and wear experiments and examines the potential of the combination of simulation and experiments on the wear mechanisms when green lubricants interact. The combination of friction and wear experiments with discrete element numerical simulations offers valuable perspectives. The electrical measurement and control systems of these machines currently integrate advanced features such as innovative sensors and multifunctional testing instruments, which have significantly improved the accuracy and efficiency of friction and wear testing. Regarding the design of combining numerical simulation and friction and wear experiments, there are still certain aspects that can be further explored:

(1) Material dimension: There is a need to broaden the research on the friction interface of the composite green lubricant system and employ discrete element simulation to analyze the formation kinetics of the composite products.
(2) Equipment dimension: The in situ diagnosis of the failure process of lubricant films can be accomplished through the combined application of servo motors and micro-area electrochemical impedance spectroscopy.
(3) Intelligent dimension: By integrating machine vision and online wear debris analysis, researchers can facilitate the upgrade of green lubrication from "passive protection" to "active response".

Author Contributions: The manuscript was written via the contributions of all authors. X.Y. wrote the original draft. D.Z. searched for literature resources. X.Y. and H.P. confirmed the final draft. B.Z. and D.L. conceptualized the study. All authors have read and agreed to the published version of the manuscript.

Funding: This research was funded by the Open Fund Project of National United Engineering Laboratory for Advanced Bearing Tribology (202401), the Fundamental Research Funds for the Central University (buctrc 202101), and the Tribology Science Fund of the State Key Laboratory of Tribology in Advanced Equipment (SKLTKF23B02).

Data Availability Statement: The data are available in a publicly accessible repository.

Conflicts of Interest: Author Haosheng Pang was employed by Chinese Aeronautical Establishment. The remaining authors declare that the research was conducted in the absence of any commercial or financial relationships that could be construed as a potential conflict of interest.

References

1. Cywar, R.M.; Rorrer, N.A.; Hoyt, C.B.; Beckham, G.T.; Chen, E.Y.X. Bio-based polymers with performance-advantaged properties. *Nat. Rev. Mater.* **2021**, *7*, 83–103. [CrossRef]
2. Zainal, N.A.; Zulkifli, N.W.M.; Gulzar, M.; Masjuki, H.H. A review on the chemistry, production, and technological potential of bio-based lubricants. *Renew. Sustain. Energy Rev.* **2018**, *82*, 80–102. [CrossRef]
3. Syahir, A.Z.; Zulkifli, N.W.M.; Masjuki, H.H.; Kalam, M.A.; Alabdulkarem, A.; Gulzar, M.; Khuong, L.S.; Harith, M.H. A review on bio-based lubricants and their applications. *J. Clean. Prod.* **2017**, *168*, 997–1016. [CrossRef]
4. Morshed, A.; Wu, H.; Jiang, Z. A Comprehensive Review of Water-Based Nanolubricants. *Lubricants* **2021**, *9*, 89. [CrossRef]
5. Rahman, M.H.; Warneke, H.; Webbert, H.; Rodriguez, J.; Austin, E.; Tokunaga, K.; Rajak, D.K.; Menezes, P.L. Water-Based Lubricants: Development, Properties, and Performances. *Lubricants* **2021**, *9*, 73. [CrossRef]
6. Hatami, M.; Hasanpour, M.; Jing, D. Recent developments of nanoparticles additives to the consumables liquids in internal combustion engines: Part II: Nano-lubricants. *J. Mol. Liq.* **2020**, *319*, 114156. [CrossRef]
7. Kotia, A.; Rajkhowa, P.; Rao, G.S.; Ghosh, S.K. Thermophysical and tribological properties of nanolubricants: A review. *Heat Mass Transf.* **2018**, *54*, 3493–3508. [CrossRef]
8. Darminesh, S.P.; Sidik, N.A.C.; Najafi, G.; Mamat, R.; Ken, T.L.; Asako, Y. Recent development on biodegradable nanolubricant: A review. *Int. Commun. Heat Mass Transf.* **2017**, *86*, 159–165. [CrossRef]
9. Ansari, F.; Sjöstedt, A.; Larsson, P.T.; Berglund, L.A.; Wågberg, L. Hierarchical wood cellulose fiber/epoxy biocomposites—Materials design of fiber porosity and nanostructure. *Compos. Part A Appl. Sci. Manuf.* **2015**, *74*, 60–68. [CrossRef]
10. Lin, L.; Ecke, N.; Kamerling, S.; Sun, C.; Wang, H.; Song, X.; Wang, K.; Zhao, S.; Zhang, J.; Schlarb, A.K. Study on the impact of graphene and cellulose nanocrystal on the friction and wear properties of SBR/NR composites under dry sliding conditions. *Wear* **2018**, *414–415*, 43–49. [CrossRef]
11. Chen, F.; Liao, Y.; Wei, S.; Zhou, H.; Wu, Y.; Qing, Y.; Li, L.; Luo, S.; Tian, C.; Wu, Y. Wood-inspired elastic and conductive cellulose aerogel with anisotropic tubular and multilayered structure for wearable pressure sensors and supercapacitors. *Int. J. Biol. Macromol.* **2023**, *250*, 126197. [CrossRef] [PubMed]
12. Shi, S.-C.; Tsai, X.-N.; Pek, S.-S. Tribological behavior and energy dissipation of hybrid nanoparticle-reinforced HPMC composites during sliding wear. *Surf. Coat. Technol.* **2020**, *389*, 125617. [CrossRef]
13. Fahs, A.; Brogly, M.; Bistac, S.; Schmitt, M. Hydroxypropyl methylcellulose (HPMC) formulated films: Relevance to adhesion and friction surface properties. *Carbohydr. Polym.* **2010**, *80*, 105–114. [CrossRef]
14. Ajmal, N.; Mohanan, V.; Pavithran, R.; Rani, S.; Thampi, A.D.; Sneha, E. Lubricant property evaluation of electrical conductive rice bran oil-based lubricant with dioctyl ammonium oleate ionic liquid as an additive. *J. Am. Oil Chem. Soc.* **2025**, *102*, 903–912. [CrossRef]
15. Hamnas, A.; Unnikrishnan, G. Green lubrication: Mustard oil-based bio-lubricant enhanced with waste eggshell-derived CaO nanoparticles for sustainable and eco-friendly industrial solutions. *J. Clean. Prod.* **2024**, *453*, 142184. [CrossRef]
16. Qin, S.; Shi, X.; Xue, Y.; Zhang, K.; Huang, Q.; Wu, C.; Ma, J.; Shu, J. Coupling effects of bionic textures with composite solid lubricants to improve tribological properties of TC4 alloy. *Tribol. Int.* **2022**, *173*, 107691. [CrossRef]
17. Huang, Q.; Shi, X.; Xue, Y.; Zhang, K.; Wu, C. Optimization of bionic textured parameter to improve the tribological performance of AISI 4140 self-lubricating composite through response surface methodology. *Tribol. Int.* **2021**, *161*, 107104. [CrossRef]
18. Zhao, F.; Zhang, L.; Li, G.; Guo, Y.; Qi, H.; Zhang, G. Significantly enhancing tribological performance of epoxy by filling with ionic liquid functionalized graphene oxide. *Carbon* **2018**, *136*, 309–319. [CrossRef]
19. Duan, H.; Li, W.; Kumara, C.; Jin, Y.; Meyer, H.M.; Luo, H.; Qu, J. Ionic liquids as oil additives for lubricating oxygen-diffusion case-hardened titanium. *Tribol. Int.* **2019**, *136*, 342–348. [CrossRef]
20. Shi, X.; Huang, W.; Wang, X. Ionic liquids–based magnetic nanofluids as lubricants. *Lubr. Sci.* **2017**, *30*, 73–82. [CrossRef]
21. Wang, H.; Che, Q.; Li, Y.; Zhang, S.; Liu, X.; Zhang, J.; Hu, L. Ionic Nitrogen-Doped Carbon Dots as Nonpolar Lubricant Additives at Low Effective Addition. *Langmuir ACS J. Surf. Colloids* **2024**, *40*, 12632–12640. [CrossRef] [PubMed]
22. Ma, R.; Li, W.; Zhao, Q.; Zheng, D.; Wang, X. In Situ Synthesized Phosphate-based Ionic Liquids as High-Performance Lubricant Additives. *Tribol. Lett.* **2019**, *67*, 60. [CrossRef]
23. Andersson, O.; Johari, G.P. Effect of pressure on thermal conductivity and pressure collapse of ice in a polymer-hydrogel and kinetic unfreezing at 1 GPa. *J. Chem. Phys.* **2011**, *134*, 124903. [CrossRef]
24. Zhang, J.; Ahn, J.-H.; Barone, P.W.; Strano, M.S.; Kim, J.-H.; Ortiz-García, R.; Yoon, H. Modulation of Single-Walled CarbonNanotube Photoluminescence by Hydrogel Swelling. *ACS Nano* **2009**, *3*, 3869–3877.

25. Mallikarjunachari, G.; Ghosh, P. Analysis of strength and response of polymer nano thin film interfaces applying nanoindentation and nanoscratch techniques. *Polymer* **2016**, *90*, 53–66. [CrossRef]
26. Yin, X.; Zhang, J.; Luo, T.; Cao, B.; Xu, J.; Chen, X.; Luo, J. Tribochemical mechanism of superlubricity in graphene quantum dots modified DLC films under high contact pressure. *Carbon* **2021**, *173*, 329–338. [CrossRef]
27. Gradt, T.; Schneider, T. Tribological Performance of MoS_2 Coatings in Various Environments. *Lubricants* **2016**, *4*, 32. [CrossRef]
28. Watanabe, S.; Noshiro, J.; Miyake, S. Friction properties of WS_2/MoS_2 multilayer films under vacuum environment. *Surf. Coat. Technol.* **2004**, *188–189*, 644–648. [CrossRef]
29. Berman, D.; Deshmukh, S.A.; Sankaranarayanan, S.K.R.S.; Erdemir, A.; Sumant, A.V. Macroscale superlubricity enabled by graphene nanoscroll formation. *Science* **2015**, *348*, 1118–1122. [CrossRef]
30. Berman, D.; Erdemir, A.; Sumant, A.V. Graphene: A new emerging lubricant. *Mater Today* **2014**, *17*, 31–42. [CrossRef]
31. Dwivedi, N.; Patra, T.; Lee, J.-B.; Yeo, R.J.; Srinivasan, S.; Dutta, T.; Sasikumar, K.; Dhand, C.; Tripathy, S.; Saifullah, M.S.M.; et al. Slippery and Wear-Resistant Surfaces Enabled by Interface Engineered Graphene. *Nano Lett.* **2020**, *20*, 905–917. [CrossRef] [PubMed]
32. Yuan, H.; Jan, A.Z.; Majeed, A.H.; Shi, L.; Kędzia, K.; Lima Ferrás, L.J.; Ali, M.R.; Hendy, A.S. Characteristics of synovial trihybrid nanofluid activation energy and Marangoni convective flow: A Computational framework of local thermal non-equilibrium. *Case Stud. Therm. Eng.* **2024**, *59*, 104519. [CrossRef]
33. Zhou, L.; Bai, J.; Liu, Y.; Liu, F.; Wang, H.; Zhang, Y.; Lu, G. Highly sensitive C_2H_2 gas sensor based on Ag modified ZnO nanorods. *Ceram. Int.* **2020**, *46*, 15764–15771. [CrossRef]
34. Zhu, Y.-P.; Wang, X.-K.; Guo, W.-L.; Wang, J.-G.; Wang, C. Sonochemical synthesis of silver nanorods by reduction of sliver nitrate in aqueous solution. *Ultrason. Sonochem.* **2010**, *17*, 675–679. [CrossRef]
35. Gao, K.; Yan, W.; Liu, Z.; Zhu, X. Wear characteristics of twin-screw extruder based on discrete element method. *China Plast.* **2023**, *37*, 135–140. [CrossRef]
36. Wang, Z.S.; Wang, R.J.; Fei, Q. Structure and Microscopic Wear Analysis of Lining Material Based on EDEM. *Int. Conf. Electron. Inf. Technol. Comput. Eng.* **2017**, *128*, 03001. [CrossRef]
37. Zhao, Q.; Dai, F.; Shi, R.; Zhao, W.; Xu, P.; Deng, H.; Pan, H. Effect of Operating Parameters on the Mulching Device Wear Behavior of a Ridging and Mulching Machine. *Lubricants* **2024**, *12*, 19. [CrossRef]
38. Zhang, Q.; Zuo, G.; Lai, Q.; Tong, J.; Zhang, Z. EDEM Investigation and Experimental Evaluation of Abrasive Wear Resistance Performance of Bionic Micro-Thorn and Convex Hull Geometrically Coupled Structured Surface. *Appl. Sci.* **2021**, *11*, 6655. [CrossRef]
39. Shojaei, A.; Arjmand, M.; Saffar, A. Studies on the friction and wear characteristics of rubber-based friction materials containing carbon and cellulose fibers. *J. Mater. Sci.* **2010**, *46*, 1890–1901. [CrossRef]
40. Tavangar, R.; Moghadam, H.A.; Khavandi, A.; Banaeifar, S. Comparison of dry sliding behavior and wear mechanism of low metallic and copper-free brake pads. *Tribol. Int.* **2020**, *151*, 106416. [CrossRef]
41. Kargarzadeh, H.; Mariano, M.; Huang, J.; Lin, N.; Ahmad, I.; Dufresne, A.; Thomas, S. Recent developments on nanocellulose reinforced polymer nanocomposites: A review. *Polymer* **2017**, *132*, 368–393. [CrossRef]
42. Wang, S.; Feng, Q.; Sun, J.; Gao, F.; Fan, W.; Zhang, Z.; Li, X.; Jiang, X. Nanocrystalline Cellulose Improves the Biocompatibility and Reduces the Wear Debris of Ultrahigh Molecular Weight Polyethylene via Weak Binding. *ACS Nano* **2015**, *10*, 298–306. [CrossRef] [PubMed]
43. Cheng, G.; Zhou, M.; Wei, Y.J.; Cheng, F.; Zhu, P.X. Comparison of mechanical reinforcement effects of cellulose nanocrystal, cellulose nanofiber, and microfibrillated cellulose in starch composites. *Polym. Compos.* **2017**, *40*, E365–E372. [CrossRef]
44. Pang, H.; Xu, J.; Liu, H.; Wang, W.; Yin, X.; Liu, D.; Zhang, B. The Induced Orientation of Hydroxypropyl Methylcellulose Coating for Ultralow Wear. *Lubricants* **2024**, *12*, 129. [CrossRef]
45. Yin, X.; Pang, H.; Yang, Y.; Hu, C.; Zhang, B. The Invention Discloses a Wear-Resistant Cellulose Coating and a Preparation Method Thereof. Patent CN202310571536.8A, 21 May 2023.
46. Pang, H.S.; Hu, C.W.; Yin, X.; Zhang, B. Experimental study on tribological properties and wear mechanism of multiscale cellulose regulated by service conditions. *J. Beijing Univ. Chem. Technol.* **2023**, *50*, 85–93. [CrossRef]
47. Mohit, H.; Selvan, V.A.M. Effect of a Novel Chemical Treatment on Nanocellulose Fibers for Enhancement of Mechanical, Electrochemical and Tribological Characteristics of Epoxy Bio-nanocomposites. *Fibers Polym.* **2019**, *20*, 1918–1944. [CrossRef]
48. Stradolini, P.; Gryczak, M.; Petzhold, C.L. Polyols from castor oil (*Ricinus communis*) and epoxidized soybean oil (*Glycine max*) for application as a lubricant base. *J. Am. Oil Chem. Soc.* **2023**, *101*, 321–334. [CrossRef]
49. Arumugam, S.; Sriram, G. Synthesis and characterisation of rapeseed oil bio-lubricant—Its effect on wear and frictional behaviour of piston ring–cylinder liner combination. *Proc. Inst. Mech. Eng. Part J J. Eng. Tribol.* **2012**, *227*, 3–15. [CrossRef]
50. Arumugam, S.; Sriram, G.; Ellappan, R. Bio-lubricant-biodiesel combination of rapeseed oil: An experimental investigation on engine oil tribology, performance, and emissions of variable compression engine. *Energy* **2014**, *72*, 618–627. [CrossRef]

51. Yao, L.; Hammond, E.G.; Wang, T.; Bu, W.; Vaknin, D. Physical and monolayer film properties of potential fatty ester biolubricants. *Eur. J. Lipid Sci. Technol.* **2014**, *116*, 910–917. [CrossRef]
52. Matiliunaite, M.; Paulauskiene, T. From concept to practice: Manufacturing of bio-lubricants from renewable resources. *Biomass Convers. Biorefinery* **2018**, *9*, 353–361. [CrossRef]
53. Bhowmik, P.; Sharma, B.K.; Sarker, M.I.; Choi, H.; Tang, C.; Roy, S. Investigating the impact of a newly developed chemical modification technique on improving the tribological properties of high oleic soybean oil. *Sustain. Energy Fuels* **2024**, *8*, 1314–1328. [CrossRef]
54. Sankaran Nair, S.; Prabhakaran Nair, K.; Rajendrakumar, P.K. Micro and nanoparticles blended sesame oil bio-lubricant: Study of its tribological and rheological properties. *Micro Nano Lett.* **2018**, *13*, 1743–1746. [CrossRef]
55. Avilés, M.-D.; Mostaza, P.; Bermúdez, M.-D.; Carrión-Vilches, F.J. Epoxidized vegetable lubricant enhanced by ionic liquid. *Wear* **2025**, *564–565*, 205740. [CrossRef]
56. Nagendramma, P. Study of pentaerythritol tetraoleate ester as industrial gear oil. *Lubr. Sci.* **2011**, *23*, 355–362. [CrossRef]
57. Li, C.; Wang, G.; Han, Q.; Feng, G.; Wang, L.; Wang, S. Effects of current-carrying conditions on lubrication and tribological performance of ionic liquid. *J. Mol. Liq.* **2022**, *367*, 120471. [CrossRef]
58. Sadeghi, M.; Omiya, T.; Fernandes, F.; Vilhena, L.; Ramalho, A.; Ferreira, F. Influence of 1-Ethyl-3-methylimidazolium Diethylphosphate Ionic Liquid on the Performance of Eu- and Gd-Doped Diamond-like Carbon Coatings. *Lubricants* **2024**, *12*, 18. [CrossRef]
59. Han, Y.; Hao, D.; Gao, P.; Wen, P.; Fan, M. Tailoring an inorganic-organic double layer tribofilm for high-performance ionic liquid magnesium alloy lubricants. *Tribol. Int.* **2023**, *179*, 108197. [CrossRef]
60. Wang, H.; Li, Y.; Zhang, S.; Che, Q.; Hu, L.; Zhang, J. Excellent corrosion inhibition and lubrication properties of carbon dot-based ionic liquids as water-based additives. *Tribol. Int.* **2023**, *189*, 108990. [CrossRef]
61. Wang, H.; Li, Y.; Zhang, S.; Che, Q.; Hu, L.; Zhang, J. Outstanding lubrication properties of carbon dot-based ionic liquids. *J. Mol. Liq.* **2023**, *376*, 121458. [CrossRef]
62. Zuo, X.; Yu, H.; Zhou, F.; Zhang, X. Synergistic Lubrication Achieved by Proton-Ionic Liquids and MoS_2 as High-Performance Water-Based Lubricant Additives. *Langmuir ACS J. Surf. Colloids* **2025**, *41*, 5534–5545. [CrossRef]
63. Li, H.; Zeng, Q.; Fan, M.; He, W.; Pang, Z.; Zhang, W. Structure-property relationship and tunable lubrication mechanism of non-covalently modified graphene oxide by imidazolium ionic liquids under molecular structure scale. *Carbon* **2025**, *238*, 120212. [CrossRef]
64. Zhang, S.; Dai, H. Simulation of nano-grinding of GaN textured surface under ionic liquids lubrication. *Mater. Today Commun.* **2024**, *39*, 109387. [CrossRef]
65. Qu, G.; Liu, L.; Fang, H.; Li, Y.; Zhang, S.; Hu, L. Exploring the distinct lubrication mechanisms of functionalized ionic liquids in air and vacuum: Insights into molecular-level behavior and performance. *Appl. Surf. Sci.* **2025**, *696*, 162955. [CrossRef]
66. Zhang, Z.; Fu, H.; Li, Z.; Huang, J.; Xu, Z.; Lai, Y.; Qian, X.; Zhang, S. Hydrogel materials for sustainable water resources harvesting & treatment: Synthesis, mechanism and applications. *Chem. Eng. J.* **2022**, *439*, 135756. [CrossRef]
67. Sun, M.; Bai, R.; Yang, X.; Song, J.; Qin, M.; Suo, Z.; He, X. Hydrogel Interferometry for Ultrasensitive and Highly Selective Chemical Detection. *Adv. Mater.* **2018**, *30*, e1804916. [CrossRef]
68. Kissel, T.; Li, Y.; Unger, F. ABA-triblock copolymers from biodegradable polyester Ablocks and hydrophilic poly(ethylene oxide) B-blocks as a candidate for in situ forming hydrogel delivery systems for proteins. *Adv. Drug Deliv. Rev.* **2002**, *54*, 99–134. [CrossRef]
69. Yan, Y.; Zhao, Y.; Wei, L.; Zhang, L.; Cui, J.; Qiu, X.; Huang, J. Load-Dependent Behavior and Underneath Mechanism of Hydrogel Friction. *ACS Appl. Polym. Mater.* **2024**, *6*, 1540–1550. [CrossRef]
70. Hafezi, M.; Qin, L.; Mahmoodi, P.; Yang, H.; Dong, G. Releasable agarose-hyaluronan hydrogel with anti-friction performance and enhanced stability for artificial joint applications. *Tribol. Int.* **2021**, *153*, 106622. [CrossRef]
71. Qin, S.Y.; Liu, X.J.; Zhuo, R.X.; Zhang, X.Z. Microstructure-Controllable Graphene Oxide Hydrogel Film Based on a pH-Responsive Graphene Oxide Hydrogel. *Macromol. Chem. Phys.* **2012**, *213*, 2044–2051. [CrossRef]
72. Zhang, Q.; Wang, Q.; Wang, G.; Zhang, Z.; Xia, S.; Gao, G. Ultrathin and Highly Tough Hydrogel Films for Multifunctional Strain Sensors. *ACS Appl. Mater. Interfaces* **2021**, *13*, 50411–50421. [CrossRef] [PubMed]
73. Hu, D.; Liu, D.; Hu, Y.; Wang, Y.; Lu, Y.; Bai, C.; Hossain, K.R.; Jiang, P.; Wang, X. Dual-physical network PVA hydrogel commensurate with articular cartilage bearing lubrication enabled by harnessing nanoscale crystalline domains. *Nano Res.* **2024**, *17*, 9784–9795. [CrossRef]
74. Lee, M.J.; Espinosa-Marzal, R.M. Intrinsic and Extrinsic Tunability of Double-Network Hydrogel Strength and Lubricity. *ACS Appl. Mater. Interfaces* **2023**, *15*, 20495–20507. [CrossRef]
75. He, X.; He, S.; Xiang, G.; Deng, L.; Zhang, H.; Wang, Y.; Li, J.; Lu, H. Precise Lubrication and Protection of Cartilage Damage by Targeting Hydrogel Microsphere. *Adv. Mater.* **2024**, *36*, e2405943. [CrossRef]

76. Ramteke, S.M.; Ramos Grez, J.; Marian, M. Enhanced mechanical and tribological performance of additively manufactured 316L steel by MoS_2-reinforcement. *Mater. Des.* **2025**, *249*, 113562. [CrossRef]
77. Fan, X.; Wei, X.; He, Y.; Zhao, Z.; Lin, K.; Zhu, M. MoS_2 functionalized lithium complex soap with enhanced thickening net structure toward high-performance thickener. *Chem. Eng. J.* **2023**, *478*, 147445. [CrossRef]
78. Boidi, G.; Zambrano, D.; Ripoll, M.R.; Rosenkranz, A. Humidity-Dependent Tribological Performance of $Ti_3C_2T_x/MoS_2$ Nanosheet-Based Hybrid Coatings. *ACS Appl. Nano Mater.* **2024**, *7*, 24947–24957. [CrossRef]
79. Zhang, Z.; Fan, X.; Ma, X.; Zhu, M. Synergistic lubrication mechanism of core/shell C@MoS_2 particles as lubricant additives. *Appl. Surf. Sci.* **2023**, *639*, 158234. [CrossRef]
80. Hu, K.H.; Hu, X.G.; Sun, X.J. Morphological effect of MoS_2 nanoparticles on catalytic oxidation and vacuum lubrication. *Appl. Surf. Sci.* **2010**, *256*, 2517–2523. [CrossRef]
81. Zhu, C.; Luo, T.; Wei, L.I.; Chen, X.; Chen, H.; Wang, Y.; Xiao, G.; Chonghai, X.U.; Cao, B. Ultrafine MoS_2 crumpled submicrosphere grown by clean laser irradiation for excellent anti-friction performance. *Tribol. Int.* **2023**, *180*, 108259. [CrossRef]
82. Zambrano-Mera, D.F.; Broens, M.I.; Villarroel, R.; Espinoza-Gonzalez, R.; Aguilar-Hurtado, J.Y.; Wang, B.; Suarez, S.; Mücklich, F.; Valenzuela, P.; Gacitúa, W.; et al. Solid lubrication performance of sandwich $Ti_3C_2T_x$-MoS_2 composite coatings. *Appl. Surf. Sci.* **2023**, *640*, 158295. [CrossRef]
83. Fan, X.; Li, X.; Zhao, Z.; Yue, Z.; Feng, P.; Ma, X.; Li, H.; Ye, X.; Zhu, M. Heterostructured rGO/MoS_2 nanocomposites toward enhancing lubrication function of industrial gear oils. *Carbon* **2022**, *191*, 84–97. [CrossRef]
84. Liao, M.; Nicolini, P.; Du, L.; Yuan, J.; Wang, S.; Yu, H.; Tang, J.; Cheng, P.; Watanabe, K.; Taniguchi, T.; et al. UItra-low friction and edge-pinning effect in large-lattice-mismatch van der Waals heterostructures. *Nat. Mater.* **2021**, *21*, 47–53. [CrossRef]
85. Wang, L.-F.; Ma, T.-B.; Hu, Y.-Z.; Zheng, Q.; Wang, H.; Luo, J. Superlubricity of two-dimensional fluorographene/MoS_2 heterostructure: A first-principles study. *Nanotechnology* **2014**, *25*, 385701. [CrossRef]
86. Yang, T.; Wang, X.; Liu, H.; Chen, S.; Liu, J.; Zhao, Q.; Gong, K.; Li, W.; Liang, Y.; Wang, X. Electrostatically Self-Assembled Magnetic Nanoparticles for High-Temperature Resistant and Friction-Controlled Lubrication System. *Small* **2024**, *20*, e2405018. [CrossRef]
87. Li, Y.; Lu, C.; Gao, K.; Zhang, Y.; Zhang, L.; Xie, G. Enhanced lubrication performance of PFPE with TMFS-modified MoS_2 under high-temperature conditions. *Appl. Surf. Sci.* **2025**, *683*, 161854. [CrossRef]
88. Long, Y.; Wang, X.; Tan, W.; Li, B.; Li, J.; Deng, W.; Li, X.; Guo, W.; Yin, J. High-Temperature Superlubricity in MoS2/Graphene van der Waals Heterostructures. *Nano Lett.* **2024**, *24*, 7572–7577. [CrossRef]
89. Yin, X.; Jin, J.; Chen, X.; Ma, T.; Zhang, C. A New Pathway for Superlubricity in a Multilayered MoS_2-Ag Film under Cryogenic Environment. *Nano Lett.* **2021**, *21*, 10165–10171. [CrossRef]
90. Liu, Q.; Wang, Y.; Bai, Y.; Li, Z.D.; Bao, M.Y.; Zhan, H.; Liu, N.; Chang, Z.D.; Ma, Y.S. Microstructural optimization and anti-wear performance of supersonic atmospheric plasma sprayed nickel based self-lubricating coatings under heavy load. *Surf. Coat. Technol.* **2021**, *421*, 127383. [CrossRef]
91. Serles, P.; Nicholson, E.; Tam, J.; Barri, N.; Chemin, J.B.; Wang, G.; Michel, Y.; Singh, C.V.; Choquet, P.; Saulot, A.; et al. High Performance Space Lubrication of MoS_2 with Tantalum. *Adv. Funct. Mater.* **2022**, *32*, 2110429. [CrossRef]
92. Song, Y.; Hinaut, A.; Scherb, S.; Pellmont, Y.; Pawlak, R.; Huang, S.; Liu, Z.; Glatzel, T.; Meyer, E. Observation of robust superlubricity of MoS_2 on Au(111) in ultrahigh vacuum. *Appl. Surf. Sci.* **2022**, *601*, 154230. [CrossRef]
93. Guo, L.; Pan, L.; Li, Z. Study on the Sliding Tribological Behavior of Oleic Acid-Modified MoS_2 under Boundary Lubrication. *Langmuir ACS J. Surf. Colloids* **2023**, *39*, 14562–14572. [CrossRef] [PubMed]
94. Babuska, T.F.; Dugger, M.T.; Walczak, K.A.; Lu, P.; Schwartzberg, A.; Aloni, S.; Kuykendall, T.R.; Curry, J.F. Tribological behavior of few-nanometer-thick MoS_2 prepared by low-temperature conversion of atomic layer deposited MoO_x films. *Surf. Coat. Technol.* **2023**, *471*, 129884. [CrossRef]
95. Behrens, B.-A.; Poll, G.; Möhwald, K.; Schöler, S.; Pape, F.; Konopka, D.; Brunotte, K.; Wester, H.; Richter, S.; Heimes, N. Characterization and Modeling of Nano Wear for Molybdenum-Based Lubrication Layer Systems. *Nanomaterials* **2021**, *11*, 1363. [CrossRef]
96. Rodríguez Ripoll, M.; Tomala, A.; Gabler, C.; Dražić, G.; Pirker, L.; Remškar, M. In situ tribochemical sulfurization of molybdenum oxide nanotubes. *Nanoscale* **2018**, *10*, 3281–3290. [CrossRef]
97. Michalczewski, R.; Ripoll, M.R.; Tomala, A.M. Tribological synergy between classical ZDDP and innovative MoS_2 and MoO_3 nanotube additives at elevated temperatures. *Proc. Est. Acad. Sci.* **2019**, *68*, 178–184. [CrossRef]
98. Yin, X.; Wu, F.; Chen, X.; Xu, J.; Wu, P.; Li, J.; Zhang, C.; Luo, J. Graphene-induced reconstruction of the sliding interface assisting the improved lubricity of various tribo-couples. *Mater. Des.* **2020**, *191*, 108661. [CrossRef]
99. Berman, D.; Deshmukh, S.A.; Sankaranarayanan, S.K.R.S.; Erdemir, A.; Sumant, A.V. Extraordinary Macroscale Wear Resistance of One Atom Thick Graphene Layer. *Adv. Funct. Mater.* **2014**, *24*, 6640–6646. [CrossRef]
100. Berman, D.; Erdemir, A.; Sumant, A.V. Few Layer Graphene to Reduce Wear and Friction on Sliding Steel Surfaces. *Carbon* **2013**, *54*, 454–459. [CrossRef]

101. Marchetto, D.; Feser, T.; Dienwiebel, M. Microscale study of frictional properties of graphene in ultra high vacuum. *Friction* **2015**, *3*, 161–169. [CrossRef]
102. Shi, J.; Ma, G.; Li, G.; Yong, Q.; Guo, W.; Xing, Z.; Wang, H. Tribological behavior of graphene/DLC coatings after AO and UV irradiation in vacuum environment. *Mater. Lett.* **2023**, *349*, 134760. [CrossRef]
103. Xu, H.; Zang, J.; Yuan, Y.; Tian, P.; Wang, Y. Preparation of multilayer graphene coatings with interfacial bond to mild steel via covalent bonding for high performance anticorrosion and wear resistance. *Carbon* **2019**, *154*, 156–168. [CrossRef]
104. Saravanan, P.; Selyanchyn, R.; Tanaka, H.; Darekar, D.; Staykov, A.; Fujikawa, S.; Lyth, S.M.; Sugimura, J. Macroscale Superlubricity of Multilayer Polyethylenimine/Graphene Oxide Coatings in Different Gas Environments. *ACS Appl. Mater. Interfaces* **2016**, *8*, 27179–27187. [CrossRef]
105. Pape, F. Investigation of Graphene Platelet-Based Dry Lubricating Film Formation in Tribological Contacts. *Coatings* **2024**, *14*, 360. [CrossRef]
106. Zhao, Z.; Fan, X.; Li, Y.; Zeng, Z.; Wei, X.; Lin, K.; Zhu, M. Well-dispersed graphene toward robust lubrication via reorganization of sliding interface. *J. Ind. Eng. Chem.* **2023**, *119*, 619–632. [CrossRef]
107. Lin, K.; Zhao, Z.; Li, Y.; Zeng, Z.; Wei, X.; Fan, X.; Zhu, M. Well-Dispersed Graphene Enhanced Lithium Complex Grease Toward High-Efficient Lubrication. *Chin. J. Mech. Eng.* **2023**, *36*, 133. [CrossRef]
108. Gan, C.; Liang, T.; Chen, D.; Li, W.; Fan, X.; Tang, G.; Lin, B.; Zhu, M. Phosphonium-organophosphate modified graphene gel towards lubrication applications. *Tribol. Int.* **2020**, *145*, 106180. [CrossRef]
109. Ghosh, G.K.; Kotia, A.; Kumar, N.; Ghosh, S.K. Multi-response Optimization of Tribological Characteristics for Graphene-Gear Oil Nanolubricants Using Grey-Taguchi Methodology Followed by Scrutinization of Lubrication Mechanisms. *J. Mater. Eng. Perform.* **2024**. [CrossRef]
110. Shi, Y.; Lin, Y.; Liu, J.; Song, W.; Zhang, C.; Chen, X.; Liu, L.; Pan, J. Tailoring the tribological properties of Cu composite coatings via integrating strengthening W particles and lubricant graphene. *Appl. Surf. Sci.* **2025**, *679*, 161248. [CrossRef]
111. Ye, W.; Zhou, Q.; Shi, Y.; Xie, M.; Chen, B.; Wang, H.; Liu, W. Robust wear performance of graphene-reinforced high entropy alloy composites. *Carbon* **2024**, *224*, 119040. [CrossRef]
112. Zheng, W.; Zhang, G.; Qi, J.; Lu, S.; Li, Y. Effect of lubricant functional groups on tribological properties of epoxy/graphene composites. *J. Appl. Polym. Sci.* **2024**, *141*, e55923. [CrossRef]
113. Nguyen, D.D.; Luo, L.-J.; Lai, J.-Y. Toward understanding the purely geometric effects of silver nanoparticles on potential application as ocular therapeutics via treatment of bacterial keratitis. *Mater. Sci. Eng. C* **2021**, *119*, 111497. [CrossRef]
114. Blackwell, S.; Smith, R.; Kenny, S.D.; Walls, J.M. Modeling evaporation, ion-beam assist, and magnetron sputtering of thin metal films over realistic time scales. *Phys. Rev. B* **2012**, *86*, 035416. [CrossRef]
115. Lee, S.L.; Beyer, T.D.; Kim, S.S.; Waldhausen, J.H.T.; Healey, P.J.; Sawin, R.S.; Ledbetter, D.J. Initial nonoperative management and delayed closure for treatment of giant omphaloceles. *J. Pediatr. Surg.* **2006**, *41*, 1846–1849. [CrossRef]
116. Taha-Tijerina, J.J.; Aviña, K.; Ulloa-Castillo, N.A.; Melo-Maximo, D.V. Thermal Transport and Physical Characteristics of Silver-Reinforced Biodegradable Nanolubricant. *Sustainability* **2023**, *15*, 8795. [CrossRef]
117. de Castilho, B.C.N.M.; Munagala, V.N.V.; Alidokht, S.A.; Sharifi, N.; Bessette, S.; Makowiec, M.E.; Gauvin, R.; Stoyanov, P.; Moreau, C.; Chromik, R.R. Insights on Silver Migration Mechanisms and their Influence on the Wear Behavior of Thermally Sprayed Self-lubricating Coatings Up to 350 °C. *Tribol. Lett.* **2022**, *70*, 120. [CrossRef]
118. Jackson, R.L.; Coker, A.B.; Tucker, Z.; Hossain, M.S.; Mills, G. An Investigation of Silver-Nanoparticle-Laden Lubricants for Electrical Contacts. *IEEE Trans. Compon. Packag. Manuf. Technol.* **2019**, *9*, 193–200. [CrossRef]
119. Hu, B.; Han, J.; Hu, N. Effect of silver-organic precursor on friction and wear. *Ind. Lubr. Tribol.* **2014**, *66*, 468–472. [CrossRef]
120. Twist, C.P.; Bassanetti, I.; Snow, M.; Delferro, M.; Bazzi, H.; Chung, Y.-W.; Marchió, L.; Marks, T.J.; Wang, Q.J. Silver-Organic Oil Additive for High-Temperature Applications. *Tribol. Lett.* **2013**, *52*, 261–269. [CrossRef]
121. Shi, X.; Xu, Z.; Wang, M.; Zhai, W.; Yao, J.; Song, S.; Qamar ud Din, A.; Zhang, Q. Tribological behavior of TiAl matrix self-lubricating composites containing silver from 25 to 800 °C. *Wear* **2013**, *303*, 486–494. [CrossRef]
122. Zhu, S.; Tan, H.; Cheng, J.; Yu, Y.; Qiao, Z.; Yang, J. Nickel Aluminum Matrix Solid-Lubricating Composite Lubricated by Silver and Silver Vanadate Formed by Tribochemistry at Elevated Temperature. *J. Tribol.* **2019**, *141*, 031302. [CrossRef]
123. Tyagi, R.; Xiong, D.S.; Li, J.; Dai, J. Elevated temperature tribological behavior of Ni based composites containing nano-silver and hBN. *Wear* **2010**, *269*, 884–890. [CrossRef]
124. Wan, H.; Jia, Y.; Ye, Y.; Xu, H.; Cui, H.; Chen, L.; Zhou, H.; Chen, J. Tribological behavior of polyimide/epoxy resin-polytetrafluoroethylene bonded solid lubricant coatings filled with in situ-synthesized silver nanoparticles. *Prog. Org. Coat.* **2017**, *106*, 111–118. [CrossRef]
125. Su, J.; Chen, J. Study on Friction and Wear Mechanisms for Coated Surface. *Mater. Heat Treat.* **2012**, *41*, 130–133.
126. Li, Y.; Zhu, P.; Tang, C.; Sun, Z. Effect of Lost-Foam Casting Process on Properties of Spiral Blade. *Crystals* **2022**, *12*, 1075. [CrossRef]

127. Hoormazdi, G.; Küpferle, J.; Röttger, A.; Theisen, W.; Hackl, K. A Concept for the Estimation of Soil-Tool Abrasive Wear Using ASTM-G65 Test Data. *Int. J. Civ. Eng.* **2019**, *17*, 103–111. [CrossRef]
128. Wang, N.; Zhao, T.; Yang, S.; Li, W.; Zhao, K. Experiment and simulation analysis on the mechanism of the spindle barrel finishing. *Int. J. Adv. Manuf. Technol.* **2020**, *109*, 57–74. [CrossRef]
129. Han, D.; Zhang, S.; Pan, Y.; Wang, C. Simulation and experimental research on the wear of synchronous quadruple rotor of an internal mixer during the mixing process. *Eng. Fail. Anal.* **2022**, *139*, 106450. [CrossRef]
130. Cundall, P.A. A computer model for simulating progressive large scale movements in blocky rock systems. In Proceedings of the International Society for Rock Mechanics (ISRM), Nancy, France, 4–6 October 1971; pp. 129–136.
131. Cundall, P.A.; Strack, O.D.L. A discrete numerical model for granular assemblies. *Geotechnique* **1979**, *29*, 47–65. [CrossRef]
132. Lemos, J.V.; Hart, P.D.; Cundall, P.A. A generalized distinct element program for modelling jointed rock mass—A keynote lecture. In Proceedings of the Intenational Symposium on Fundamentals of Rock Joints, Björkliden, Sweden, 15–20 September 1985; pp. 335–343.
133. Lorig, L. A Hybrid Computational Model for Excation and Support Design in Jointed Media (Rock, Tunnel, Mining). Ph.D. Thesis, University of Minnesota, Minneapolis, MN, USA, 1984.
134. Shi, G.; Li, J.; Ding, L.; Zhang, Z.; Ding, H.; Li, N.; Kan, Z. Calibration and Tests for the Discrete Element Simulation Parameters of Fallen Jujube Fruit. *Agriculture* **2021**, *12*, 38. [CrossRef]
135. Chen, X.; Gu, F.; Hu, Z.; Wu, F.; Luo, W.; Guo, K. The Calibration of Soil Simulation Parameters for Wheat Grown after Rice in the Yangtze River Basin of China. *Sustainability* **2023**, *15*, 15079. [CrossRef]
136. Ma, Z.; Wu, Z.; Li, Y.; Song, Z.; Yu, J.; Li, Y.; Xu, L. Study of the grain particle-conveying performance of a bionic non-smooth-structure screw conveyor. *Biosyst. Eng.* **2024**, *238*, 94–104. [CrossRef]
137. Wang, Y. Discrete Element Method—A Numerical Method Suitable for Analysis in Jointed Rocks. In Proceedings of the 1st National Symposium on Numerical Calculation and Model Test of Rock Mechanics, Ji'an, China, 20–27 June 1986; pp. 32–37.
138. Gui, Y.L.; Zhao, Z.Y.; Kodikara, J.; Bui, H.H.; Yang, S.Q. Numerical modelling of laboratory soil desiccation cracking using UDEC with a mix-mode cohesive fracture model. *Eng. Geol.* **2016**, *202*, 14–23. [CrossRef]
139. Wang, Z.; Su, H.; Luo, C.; Ma, S.; Ding, H. Particle Flow Simulation of Failure Process of Defective Sandstone Under Different Intermediate Principal Stress Under True Triaxial Action. *Processes* **2022**, *10*, 2028. [CrossRef]
140. Meijs, J.W.H.; Weier, O.W.; Peters, M.J.; Oosterom, A.V. On the Numerical Accuracy of the Boundary Element Method. *IEEE Trans. Biomed. Eng.* **1989**, *36*, 1038–1049. [CrossRef]
141. Ma, Y.; Huang, H. DEM analysis of failure mechanisms in the intact Brazilian test. *Int. J. Rock Mech. Min. Sci.* **2018**, *102*, 109–119. [CrossRef]
142. Sah, R.K.; Das, A.K. Drainage skeletonization from flow-accumulated area without the use of threshold. *Geocarto Int.* **2015**, *30*, 894–904. [CrossRef]
143. Du, X.; Li, W.; Li, X.; Wang, H. The impact of digital elevation model and land use spatial information on Hydrologic Simulation Program-FORTRAN—Predicted stream flow and sediment uncertainty. *J. Hydroinformatics* **2014**, *16*, 989–1003. [CrossRef]
144. Liang, S.; Feng, Y.T.; Wang, Z. Numerical methods and key issues for the study of particle material fragmentation behavior—A review. *Powder Technol.* **2025**, *451*, 120457. [CrossRef]
145. Piska, R.; Sivadas, K.; Boyina, K.; Vuppuluri, A.; Chaurasia, A.; Parimi, C.; Rabczuk, T. Recent trends in computational damage models: An overview. *Theor. Appl. Fract. Mech.* **2024**, *132*, 104494. [CrossRef]
146. Urrea-Quintero, J.-H.; Marino, M.; Wick, T.; Nackenhorst, U. A Comparative Analysis of Transient Finite-Strain Coupled Diffusion-Deformation Theories for Hydrogels. *Arch. Comput. Methods Eng.* **2024**, *31*, 3767–3800. [CrossRef]
147. Lv, J.; Li, K.; Slowik, A.; Jiang, H. Distributed Edge Intelligence for Rapid In-Vehicle Medical Emergency Response in Internet of Vehicles. *IEEE Internet Things J.* **2025**, *12*, 4750–4760. [CrossRef]
148. Li, X.; Yang, Y.; Liu, D.; Chen, S.; Wu, S.; Yuan, X.; Liu, Z.; Wang, Y.; Zhang, H. Optimization of recirculating water scallop larval cultivation system based on EDEM-fluent coupling. *Front. Mar. Sci.* **2024**, *11*, 1407670. [CrossRef]
149. Li, C.; Li, Z.; Wang, T.; Ling, G.; Wang, S.; Li, J. Parameter optimization of column-comb harvesting of litchi based on the EDEM. *Sci. Hortic.* **2023**, *321*, 112216. [CrossRef]
150. Chen, G.; Schott, D.L.; Lodewijks, G. Sensitivity analysis of DEM prediction for sliding wear by single iron ore particle. *Eng. Comput.* **2017**, *34*, 2031–2053. [CrossRef]
151. Liu, X.; Du, C.; Fu, X.; Zhao, H.; Zhang, J.; Yang, X. Wear analysis and performance optimization of drum blade in mining coal gangue with shearer. *Eng. Fail. Anal.* **2021**, *128*, 105542. [CrossRef]
152. Yang, W.; Meng, W.; Gao, L.; Tan, Y.; Fottner, J.; Dai, X.; Yao, F.; Yuan, Y.; Sun, X. Analysis of the Screw Flight Wear Model and Wear Regularity of the Bulk Transport in Screw Ship Unloader. *Iran. J. Sci. Technol. Trans. Mech. Eng.* **2021**, *46*, 15–29. [CrossRef]
153. Pang, H.; Yang, Y.; Yin, X.; Zhang, B. Experimental and simulation study of a grinding screw surface based on cross-viscosity cellulose. *J. Beijing Univ. Chem. Technol.* **2024**, *51*, 67–75. [CrossRef]

154. Yin, X.; Zhang, D.; Li, L.; Zhang, B. The Influence of Length-Diameter Ratio of Cellulose on Friction Characteristics of Screw Surface Investigated by EDEM Simulation. *Macromol. Theory Simul.* **2024**, *34*, 2400083. [CrossRef]
155. Wang, Y. Design and Experimental Study of Multifunction Tribometer. Master's Thesis, Yangzhou University, Yangzhou, China, 2023.
156. Alshkane, Y.M.; Marshall, A.M.; Stace, L.R. Prediction of strength and deformability of an interlocked blocky rock mass using UDEC. *J. Rock Mech. Geotech. Eng.* **2017**, *9*, 531–542. [CrossRef]
157. Wu, Z.; Luo, S.; Go, Z.; Li, W. *Mechanical Design Course Design Manual*, 5th ed.; Higher Education Press: Beijing, China, 2018.
158. Xu, J. Development of Tribological Experimental Device and Research on Tribological Properties. Master's Thesis, China Academy of Machinery Wuhan Research Insititute of Materials Protection, Wuhan, China, 2013.
159. Santner, D.E. Laboratories at work: Tribology at BAM. *Tribotest* **1994**, *1*, 77–89. [CrossRef]
160. Pape, F.; Gatzen, H.-H.; Poll, G. Micro Tribological Investigations on Dry Sliding Friction of 100Cr6 Axial Bearing Surfaces. *Tribol. Online* **2016**, *11*, 547–550. [CrossRef]
161. Ma, G.; Xu, B.; Wang, H.; Si, H. Study and Discussion on the Development of Special Friction and Wear Testing Machine. *Eng. Test* **2009**, *49*, 1–5.
162. Lanzhou Institute of Chemical Physics (Chinese Academy of Sciences). Development of HT-500 high temperature friction and wear testing machine. *Surf. Eng. Inf.* **2005**, *5*, 13.
163. Duranty, E.R.; Roosendaal, T.J.; Pitman, S.G.; Tucker, J.C.; Owsley, S.L.; Suter, J.D.; Alvine, K.J. An in situ tribometer for measuring friction and wear of polymers in a high pressure hydrogen environment. *Rev. Sci. Instrum.* **2017**, *88*, 95114. [CrossRef]
164. Zhang, T.; Jiang, F.; Yan, L.; Jiang, Z.; Xu, X. A novel ultrahigh-speed ball-on-disc tribometer. *Tribol. Int.* **2021**, *157*, 106901. [CrossRef]
165. Ma, G.; Xu, B.; Wang, H.; Zhang, S. Development of a Novel Multifunctional Vacuum Tribometer. *Chin. J. Vac. Sci. Technol.* **2013**, *33*, 162–167.
166. Francis, E.K.; Youxiong, Y.; Ian, B.; Raina, R.W.; Robert, L.B.; Aubrey, Y.T.; Min, S. Development of a new cryogenic tribotester and its application to the study of cryogenic wear of AISI 316 stainless steel. *Wear* **2022**, *496*, 204309. [CrossRef]
167. Zhang, L. Development and Performance Analusis of Controlled Atmosphere Friction and Wear Testing Machine. Master's Thesis, Xi'an University of Technology, Xi'an, China, 2018.
168. Cheng, P. Intelligent Measurement and Control System of the Multifunctional Environment Controllable Tribometer. Master's Thesis, Hefei University of Technology, Hefei, China, 2008.
169. Wei, B.; Yin, X.; Li, L.; Zhang, B.; Ma, C. The Utility Model Relates to a Face-Surface Rotating Functional Material Testing Machine. CN202311081964.9A, 26 August 2023.
170. Shen, Z.; Guo, F.; Ding, H. *Modern Test Technology and System Design*; Xi'an Jiaotong University Press: Xi'an, China, 2006; pp. 79–97.
171. Jian, K. Reciprocating Friction and Wear Test Rig Control System Design. Master's Thesis, Northeastern University, Shenyang, China, 2011.
172. Liu, L. Development of Reciprocating Friction and Tear Testing Machine. Master's Thesis, Lanzhou University of Technology, Lanzhou, China, 2006.
173. Chai, J.; Zhou, Z.; Ye, C.; Yao, C.; Li, G. Design and development of a novel sliding friction and wear tester with complex working conditions. *Sci. Rep.* **2021**, *11*, 6903. [CrossRef]

Disclaimer/Publisher's Note: The statements, opinions and data contained in all publications are solely those of the individual author(s) and contributor(s) and not of MDPI and/or the editor(s). MDPI and/or the editor(s) disclaim responsibility for any injury to people or property resulting from any ideas, methods, instructions or products referred to in the content.